# National and Technical University of Athens

# Delft University of Technology
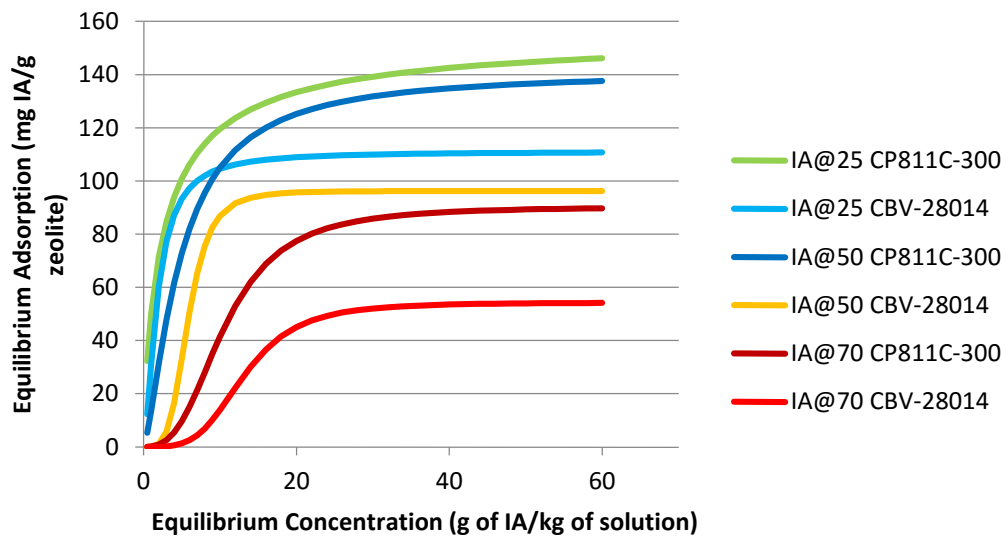
**National Technical University of Athens**

**Technische Universiteit Delft**

# MASTER THESIS

# Hydrophobic adsorption of itaconic and fumaric acid on high silica zeolites



## Ioannis-Panagiotis Kipouros

**TU Delft Student Number:** 4430573

**Daily Supervisor:** Ir. E.B.G. Häusler

**Supervisor:** Dr. Ir. A.J.J Straathof

**Home University Supervising Professor:** Antonios Kokossis

**Home University Student Number:** 05110084

# Abstract

The oil crisis in the 70's and more recently the surging oil prices and concerns about the depleting petroleum reserves, have prompted the development of bio – production processes for bio – based chemical feedstocks as an alternative to petrochemically – based ones. Many dicarboxylic acids, including fumaric acid, malic acid, succinic acid and itaconic acid have been identified as top building-block chemicals that potentially can be produced from abundant renewable biomass [2]. Adsorption is a chemical process considered for their purification. Modelling of experimental adsorption isotherm data is an indispensable tool to predict the nature and the mechanisms of adsorption, which, consequently, will lead to a significant improvement in the field of adsorption science. In this work six isotherm models, namely: Langmuir (single and double site), Freundlich, Sips, Toth, Redlich – Peterson, were investigated to correlate several experimental sets of adsorption data including four different compounds (itaconic, fumaric, malic, citric acid) at three different temperatures (25, 50 and 70ºC) on two different zeolites, CBV28014 and CP811C-300. In this work the applicability of adsorption of these compounds on zeolites was tested as a means of removal from aqueous phase with the aim of extending to fermentation broths and other applications. Only nonlinear regression methods were applied. Sum of squared errors of prediction (SSE) was used to determine the best – fit parameters to every model investigated and five error functions, adjusted correlation coefficient ($R^2$), nonlinear chi-square test ($\chi^2$), hybrid fractional error function (HYBRID), average relative error (ARE) and Marquardt's percent standard deviation (MPSD) were used to evaluate the best – fitting equilibrium model to the experimental data. The modeling results showed that non-linear Sips equation model could fit the data better than others, with relatively higher $R^2$ values and smaller (ARE), but that was not always the case. At certain cases, more than one model fit well enough, so a definite conclusion could be achieved by carrying out more experiments in the lowest, especially, concentration range for each compound.

# Table of Contents

# 1. Introduction

## 1.1. Renewable resources

During the last years due to the constantly increasing prices of fossil feedstock and fossil fuels fementatively bio produced chemical compounds have brought back the interest in their production by renewable resources and could turn out to be a cheaper alternative to the currently used petrochemically – based ones. Some dicarboxylic acids such as itaconic and fumaric acid are considered to be promising raw materials [2] in the polymer industry and therefore interest is raised not only in fermentation processes for production of these compounds from alternative feedstocks, but also in increasing yield of the overall process.

## 1.2. Itaconic and fumaric acid

Itaconic acid or methylenesuccinic acid is a dicarboxylic acid and it is a white crystalline powder. It is a naturally occurring compound, non-toxic and biodegradable with the formula $C_5H_6O_4$. Fumaric acid or trans-butenedioic acid is also a dicarboxylic acid, with the formula $C_4H_4O_4$. It is white and crystalline and it is one of the 2 isomeric unsaturated acids, the other one is maleic acid. Its taste is fruity and the salts and its salts and esters are called fumarates. The molecular structure and some characteristics of these compounds can be seen in Figure 1,, Figure 2, Figure 3 and Figure 4 and in Table 1. A general overview can be seen in Figure 5 :
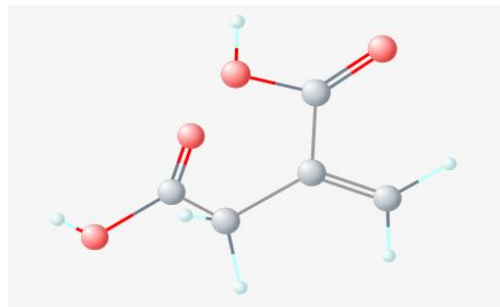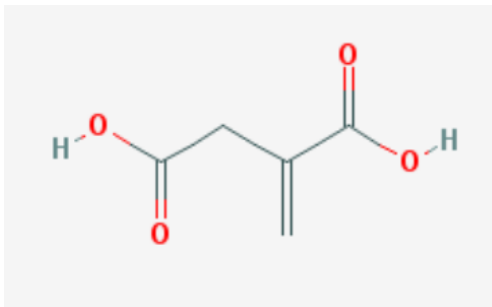


Figure 1: 2-D molecular structure of Figure 2: 3-D molecular structure of itaconic acid
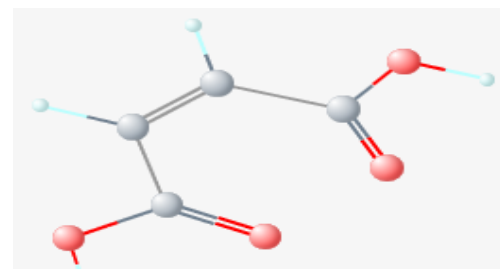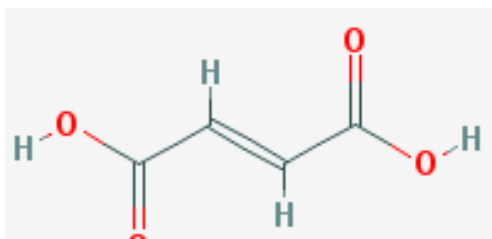


Figure 4: 2-D molecular structure of ftFigure 3: 3-D molecular structure of fumaric acid

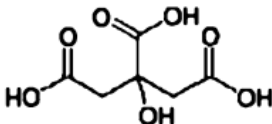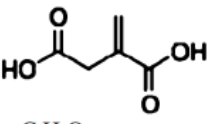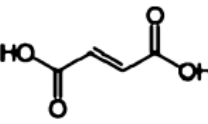| Common name | Itaconic acid | Fumaric acid |
|---|---|---|
| IUPAC name | 2-methylidenebutanedioic acid | (E)-but-2-enedioic acid |
| CAS number | 97-65-4 | 110-17-8 |
| Molecular formula | $HOOCCH_2C(=CH_2)COOH$, $C_5H_6O_4$ | $HO_2CCH=CHCO_2H$, $C_4H_4O_4$ |
| Molar Mass | 130.026609 g/mol | 116.072 g/mol |
| Boiling point | 268°C | $\geq$ 200°C |
| Melting point | 165 – 169°C | 287°C |
| pKa | 3.84 and 5.55 ($pKa_1$ and $pKa_2$) | 3.03 and 4.44 ($pKa_1$ and $pKa_2$) |
| Solubility | Water: 1 g/12 ml | Water: 4.3 g/L (20°C) |
| | Ethanol: 1 g/5 ml | |
| Density | 1.632 g/L (20°C) | 1.635 g/L (20°C) |
| Estimated market value | 126.4 Million USD $ in 2014, 204.6 Million USD $ by 2023 | 764.8 Million USD $ by 2020 |
| Price | Production: 0.5 USD $ | - |
| | Sale: 2 USD $ | - |
| Log(Kow) | 0.05 | 0.46 |



| | Citric Acid | Itaconic Acid | Fumaric Acid | Malic Acid |
|---|---|---|---|---|
| Molecular structure and formula | $C_6H_8O_7$ | $C_5H_6O_4$ | $C_4H_4O_4$ | $C_4H_6O_5$ |
| Molar mass (g/mol) | 192.1 | 130.1 | 116.1 | 134.1 |
| Density (g/cm³) | 1.665 | 1.632 | 1.635 | 1.609 |
| Solubility in water (g/100 mL, 20°C) | 73 | 8.31 | 0.63 | 55.8 |
| Acidity (pKa) | $pK_{a1}$ = 3.09 $pK_{a2}$ = 4.75 $pK_{a3}$ = 6.41 | $pK_{a1}$ = 3.84 $pK_{a2}$ = 5.55 | $pK_{a1}$ = 3.03 $pK_{a2}$ = 4.44 | $pK_{a1}$ = 3.40 $pK_{a2}$ = 5.20 |
| Applications | Food, beverages, pharmaceuticals, detergents; buffering and chelating agents | Bioactive compounds in agriculture and medicine; polymer intermediate; coating, plasticizer | Food acidulant; feed additive; medicine; raw material for polyester resins, polyhydric alcohols | Food, beverages, nutrition supplement, polymer intermediate |
| Production methods | Aerobic fermentation with *A. niger* | Aerobic fermentation with *A. terreus* | Catalytic isomerization of maleic acid derived from maleic anhydride, which is produced from *n*-butene via catalytic oxidation | Catalytic hydration of maleic or fumaric acid |
| Annual production (metric ton) | 1,600,000 | 80,000 | 90,000 | 200,000 |
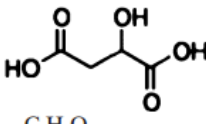
Figure 5: Properties and applications of citric, itaconic, fumaric and malic acid [9]

Other names and/or synonyms of the IA are: methylene succinic acid, Methylene Butanedioic acid, Propylene dicarboxylic acid and 2-Propene-1, 2-dicarboxylic acid.

Both of these dicarboxylic acids along with the rest of the compounds on Figure 5 are promising biomass – based chemical platforms for the future and their role is very important in the production of a variety of polymers that have a lot of applications in the fields of chemistry, pharmacy, agriculture, resins and paints. From now on, every compound will be referred to with its initials, namely itaconic acid as IA, fumaric acid as FA, malic acid as MA and citric acid as CA.

### 1.2.1. Production Process and Utilization

IA can be not only chemically, but also biotechnologically produced. The current process involves fermentation of 1st generation sugars (Figure 6) which do not require pretreatment such as sucrose and glucose using the fungus *Aspergillus Terreus*. Fungal fermentation of glucose gives final product concentrations up to 100 g/L at low pH and IA is recovered from fermentation broth by
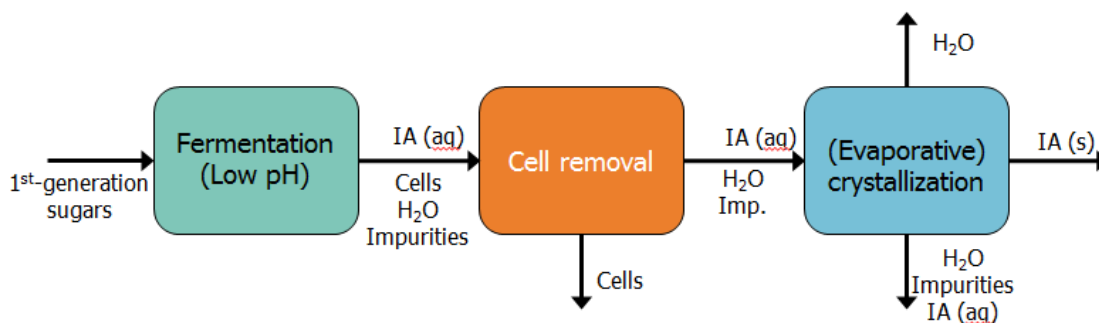


**Figure 6: Current IA production process (Erik B.G. Häusler, Department of Biotechnology, TU Delft, Extraction for recovery of IA)**

evaporative crystallization [10], but yields are low (0.34 g/g) and productivity has never exceeded 1 g/L·h, with the final product concentration of less than 80 g/L [9] because of impurities in the aqueous phase [11] such as residual glucose (raw material), other carboxylic acid and salts. FA was first isolated from the plant *Fumaria officinalis* (its name is derived from this plant) and it is a key to the citrate cycle. Many microorganisms produce FA, but it is in small amounts. Nowadays, FA is produced by chemical synthesis from maleic anhydride. More precisely, FA is produced by isomerization of maleic acid, which is produced from maleic anhydride. Maleic anhydride, in turn, is industrially produced by catalytic oxidation of specific hydrocarbons in the gas phase. Benzene used to be the dominant starting material, but oxidation of *n*-butane or *n*-butane–*n*-butene mixtures has become more popular in recent



**Figure 7: Current applications of FA production [1]**

years (Lohbeck et al. 1990). The butane oxidation reaction equation to maleic anhydride is: $C_4H_{10} + 3.5O_2 \rightarrow C_4H_2O_3 + 4H_2O$. In Figure 7 some of the application of FA can be seen. Production by the fungus *filamentus fungi* has been reviewed (Magnuson and Lasure 2004; Goldberg et al. 2006), but the microorganism with the highest productivity is *rhizopus oryzae,* which is capable of producing FA with an average yield of 85 g/liter from 100 g of glucose per liter within 20hours under repetitive fed-batch cycles. On a weight yield basis, 91% of the theoretical maximum was obtained with a productivity of 4.25 g/liter/h [12]. The production process contains the combination of two pathways, the citrate cycle and the reductive pyruvate carboxylation. Of course, the productivity of the process is determined by
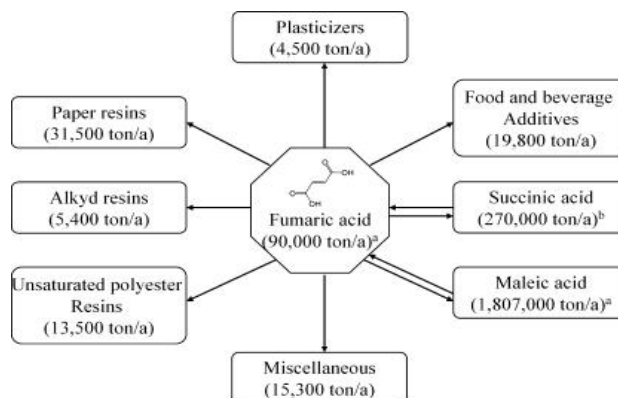
many aspects such as the use of neutralizing agent, the applied microbial strain and the applied feedstock. [13], [1]

Both IA and FA are biotechnologically produced by fermentation of different microbial strains. In order for these substances to be commercially exploitable and gain added value, product isolation, namely removal of those components whose properties vary markedly from that of the desired product as well as product purification, a process done to separate those contaminants that resemble the product very closely in physical and chemical properties are essential. These 2 processes are part of the so called downstream processing (DSP), which mainly refers to the recovery and purification of biosynthetic products from e.g. a fermentation broth. Thereafter, adsorption could be an efficient method to recover both itaconic and fumaric if the selective adsorption of the non-dissociated form of acids from the fermentation media is achieved and consequently no other components are inserted into the solution. This way, the recovery is easier and less energy consuming since no extra separation step is required. A way to achieve that is by exploiting hydrophobic interactions in IA and FA separations. Despite the fact that these acids have two polar carboxylic groups, the presence of the carbon chain could be effective concerning their hydrophobic capture. High silica zeolites can be utilized to adsorb non-dissociated acid species based on their hydrophobicity. If it is taken into consideration that in the future currently used carbon sources (glucose) are probably going to be substituted by biomass-based feedstock (lignocellulosic) leading to higher level of impurities, economic efficiency (yield) of the process has to be increased in order for these compounds to be a realistic alternative to petrol-based compounds in industry. Therefore, a capture purifying step before evaporative crystallization is proposed, hydrophobic adsorption on zeolites [14], [15] and consequently hydrophobic adsorption of IA and FA from low pH fermentation medium by high silica zeolites will be further investigated below [16].

## 1.3. Adsorption

### 1.3.1. Definition

Adsorption is the adhesion of molecules of gas, liquid, or dissolved solids to a surface. The term also refers to a method of treating wastes in which activated carbon is used to remove organic compounds from wastewater [17] . In other words, adsorption is a process that occurs when a gas or liquid solute accumulates on the surface of a solid or a liquid (adsorbent), forming a molecular or atomic film (the adsorbate). It is different from absorption, in which a substance diffuses into a liquid or solid to form a solution. The term sorption encompasses both processes, while desorption is the reverse process.
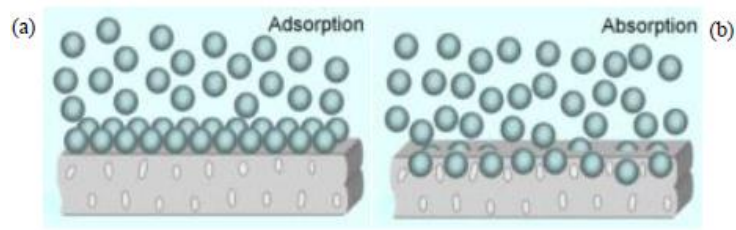
Adsorption is applicable in most natural physical, biological, and chemical systems and is widely used in industrial applications such as activated charcoal, synthetic resins and water purification. Similar to surface tension, adsorption is a consequence of surface energy. In a bulk material, all the bonding requirements (be they ionic, covalent or metallic) of the constituent atoms of the material are filled. But atoms on the (clean) surface experience a bond deficiency, because they are not wholly surrounded by other atoms. Thus it is energetically favorable for them to bond with whatever happens to be available. The exact nature of the bonding depends on the details of the species involved, but the adsorbed material is generally classified as exhibiting physisorption or chemisorption.

Two types of (ad) sorption are distinguished:

Physisorption or physical adsorption is this type of adsorption in which the adsorbate adheres to the surface only through Van der Waals (weak intermolecular) interactions, which are also responsible for the non-ideal behavior of real gases. The adsorption energy is typically less than 0.3 eV per adsorbate particle (6.9 Kcal/mol) and there is no covalent bond.

Chemisorption is a type of adsorption whereby a molecule adheres to a surface through the formation of a chemical bond which results in the modification of the adsorbate's electronic structure. As opposed to the Van der Waals forces which cause physisorption, here, the adsorption energy is larger. For chemisorption systems there is a further classification of the nature of bonding, based on electronic, electrical, vibrational and thermal properties. Altogether there are four different types of bonding: 1) Van der Waals, 2) Covalent, 3) Metallic and 4) Ionic. [18]

Adsorption is usually described through isotherms, that is, functions which connect the amount of adsorbate on the adsorbent, with its pressure (if gas) or concentration (if liquid). Several models (Freundlich, Langmuir, BET isotherm) can be found describing the process some of which are going to be discussed below.

### 1.3.2. Adsorption isotherm models

Generally, an adsorption isotherm is a unique curve describing the phenomenon controlling the retention (or release) of a substance from the aqueous porous media or aquatic environments to a solid-phase at a constant temperature and pH [19], [20]. Adsorption equilibrium, defined as the ratio between the adsorbed amounts with the remaining ones in the solution, is established when an adsorbate containing phase has been contacted with the adsorbent for sufficient time, with its adsorbate concentration in the bulk solution is in a dynamic balance with the interface concentration [21]. Usually, the mathematical correlation, which proves to play an indispensable role towards the modelling of the system and its operational design, is usually expressed by depicting the binding capacity against the equilibrium concentration [22].

Since the adsorptive and the adsorbent often undergo a chemical reactions, the chemical and physical properties of the adsorbate is not always just the sum of the individual properties of the adsorptive and the adsorbent and often represents a phase with new properties. The physicochemical parameters along with the thermodynamic assumptions provide an insight into the mechanism, surface properties as well as the degree of affinity of the adsorbents.
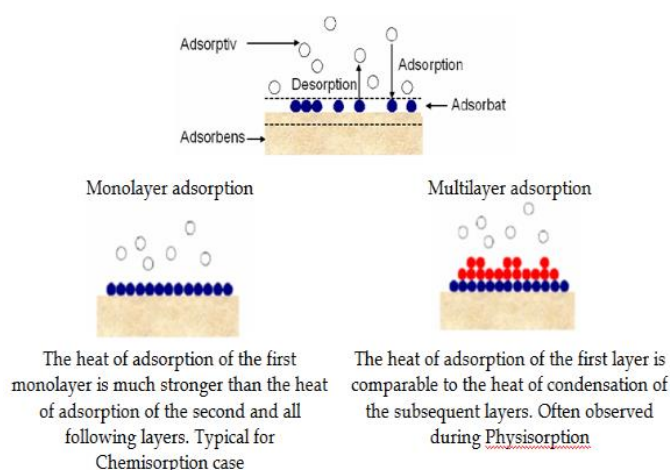


**Figure 9: K. Christmann, 2010 Adsorption. Lecture Series 2010/2011: "Modern Methods in Heterogeneous Catalysis Research", Institut für Chemie und Biochemie, Freie Universität, Berlin**

Adsorption of molecules itself on a specific adsorbent is uniquely characterized by the respective isotherm. Generally, molecules tend to be adsorbed at different levels for different initial concentrations. Zeolites and each adsorbent has a specific different capacity for a given molecule and this capacity is depending on the size of the molecule and the available sites. The sites, depending on the type of interaction between the molecule and the adsorbent, can be ion exchange sites for ion exchange resins (Polystyrene sulfonates) e.g. water softening using a sodium cation exchange resin, hydrophobic sites for hydrophobic interaction (adsorption of hydrophobic pollutants using activated carbon and [23]) , and hydrophilic sites for hydrophilic interaction (adsorption of proteins on hydrophilic surfaces [24], [25]. More than one adsorption site can be present in the same adsorbent. The amount of adsorbent adsorbed is represented by the loading ($q$ in g/unit amount of adsorbent) and the maximum achievable loading is

represented with $q_{max}$. The affinity of the molecule towards the adsorbent is defined by the affinity coefficient ($K_{so}$ inverse of concentration unit) which is a function of the heat of adsorption of the molecule.

Modelling of adsorption processes is not as straightforward as conventional separation processes like distillation. Therefore, the scale up of the adsorption processes requires well defined mathematical models that represent the system efficiently. A suitable model should have the right parameters that define the system precisely. Most of these parameters can be estimated from batch experiments. There are numerous mathematical models listed in literature [26] that can describe the relation and interactions between an adsorbate – adsorbent pair such as Langmuir, Sips, BET, Tempkin, Hill, Flory – Huggins, Toth. The choice of these isotherms was not random. Based on literature [27], [28], when investigating the applicability of adsorption isotherm models on zeolites, Freundlich, Single Langmuir and Redlich – Peterson are typically used to describe the interactions between adsorbent and adsorbate

In this work, 3 additional adsorption isotherms (Table 2) have been chosen to be investigated and to be compared to the experimental data to determine which one of them best fits. Since Sips is a combination of Freundlich and single Langmuir and it is not usually investigated and Toth is an empirical equation developed to improve single Langmuir isothermal fittings (see below), these two isotherms were also chosen to be included to the evaluation process.

**Table 2: Adsorption isotherms along with their equations that were investigated [26]**

| Isotherm | Nonlinear form | Parameters | |
|---|---|---|---|
| **Freundlich** | $q_e = K_F C_e^{1/n}$ | $K_F, n$ | (1) |
| **Single Langmuir** | $q_e = \dfrac{q_{sat} k_L C_e}{1 + k_L C_e}$ | $q_{sat}, k$ | (2) |
| **Double Langmuir** | $q_e = \dfrac{q_{sat,A} k_A C_e}{1 + k_A C_e} + \dfrac{q_{sat,B} k_B C_e}{1 + k_B C_e}$ | $q_{satA}, k_A, q_{satB}, k_B$ | (3) |
| **Sips** | $q_e = \dfrac{K_s C_e^{\beta_S}}{1 + a_S C_e^{\beta_S}}$ | $K_s, \beta_S, \alpha_S$ | (4) |
| **Toth** | $q_e = \dfrac{K_T C_e}{(\alpha_T + C_e)^{1/t}}$ | $K_T, \alpha_T, t$ | (5) |
| **Redlich Peterson** | $q_e = \dfrac{K_R C_e}{1 + \alpha_R C_e^g}$ | $K_R, \alpha_R, g$ | (6) |

## Freundlich

Freundlich isotherm is a relationship known for describing the non-ideal, reversible and not restricted to the formation of monolayer adsorption. It is an empirical model that can be also applied to multilayer adsorption with non – uniform distribution of heat and affinities. The equation describes the amount

adsorbed as a summation of adsorption on all sites, where the stronger binding sites are occupied first until the adsorption energy is exponentially decreased upon the completion of the adsorption process.

As far as its applications are concerned, it is widely applied in heterogeneous systems. The slope, $n$, which ranges from 0 to 1, is a unitless measure of adsorption intensity or surface heterogeneity (close to 0, more heterogeneous). Values below unity imply chemisorption processes, whereas values of $1/n$ above unity imply cooperative adsorption. $K_F$ is a constant (mg/g) (kg/g)$^n$ related to adsorption capacity. [29], [30], [31], [32]

## Single site Langmuir

Langmuir adsorption isotherm was initially developed to predict gas – solid phase adsorption onto activated carbon. This empirical model assumes monolayer adsorption, which practically means that the adsorption layer is one molecule in thickness, and as a result adsorption can only occur at a fixed number of identical equivalent local sites. Graphically, the isotherm is characterized by a typical plateau, a saturation point where once a molecule has occupied a site no further adsorption can take place. [33], [34], [35]. It is a 2 parameter equation, where $q_{sat}$ or $q_{max}$ is a constant related to the maximum monolayer coverage capacities (mg/g) and $k_L$ is a Langmuir isotherm constant (kg/g). A dimensionless constant can also be defined by Webber and Chakkravorti, known as separation factor $R_L$, represented as:

$$R_L = \frac{1}{1 + k_L C_o} \tag{7}$$

, where if

- $R_L = 0$, irreversible adsorption
- $R_L = 1$, linear adsorption
- $0 < R_L < 1$ favorable
- $R_L > 1$, unfavorable

## Double Site Langmuir

Sometimes the adsorption of molecules on zeolite adsorbents is best described by a dual site Langmuir isotherm. There are different descriptions for the dual site adsorption behavior. One theory states that linear molecules are adsorbed on the channel walls. However, when the molecules are branched they can also adsorb on the channel crossings due to their molecular orientation and this is how a second adsorption site is generated. Another description states that during normal loading the molecules are located in the main channels while during high loading the molecules also diffuse into narrower channels. [16]. Double site Langmuir is a 4 parameter equation, $q_{sat,A}, k_A, q_{sat,B}, k_B$ where constants are the same as in single Langmuir with the only difference that here there are 2 adsorption sites.

## Sips

Sips isotherm is a combined mathematical form of both single site Langmuir and Freundlich equations. It is mainly used to describe heterogeneous adsorption systems and it can well circumvent the limitations

related to the rising adsorbate concentration (Freundlich model). It is a 3 parameter equation, where $a_S$ is a Sips isotherm model constant (kg/g), $K_S$ is another Sips isotherm model constant (g/g) and $\beta_S$ is a Sips isotherm model exponent. From its mathematical expression, at low adsorbate concentrations, it reduces to Freundlich isotherm, while at high concentrations, it predicts a monolayer adsorption capacity similar to the one predicted by Langmuir [36], [37]

### Toth

Toth isotherm model is an empirical three parameter equation, where $a_T$ is an isotherm constant (g/kg), $K_T$ is also an isotherm constant (g/g) and $t$ is the third isotherm constant. The main reason for its development was to improve Langmuir isothermal fittings. It is usually used to describe heterogeneous systems satisfying both low and high-end boundary concentration. [38], [33]

### Redlich – Peterson

Redlich – Peterson equation is a hybrid isotherm also featuring, just like Sips, both Langmuir and Freundlich isotherms, incorporating three parameters, $a_R$ an isotherm constant (kg/g), $K_R$ an isotherm constant (g/g) and g an isotherm unitless exponent into an empirical equation. From its mathematical expression, the model has a linear dependence on concentration in the numerator and an exponential function in the denominator. By this way, it represents a wide range of concentrations and therefore it can be applied to both homo- and heterogeneous systems. [39], [40]

## 1.4.    Zeolites

Zeolites are hydrated aluminosilicate ($Al_2$ and $Si$) minerals and have a micro-porous structure. They are part of the of microporous solids known as "molecular sieves." The term molecular sieve refers to a particular property of these materials, i.e., the ability to selectively sort molecules based primarily on a size exclusion process. This is due to a very regular pore structure of molecular dimensions. The maximum size of the molecular or ionic species that can enter the pores of a zeolite is controlled by the dimensions of the channels. These are conventionally defined by the ring size of the aperture, where, for example, the term "8-ring" refers to a closed loop that is built from eight tetrahedrally coordinated silicon (or aluminum) atoms and 8 oxygen atoms. These rings are not always perfectly symmetrical due to a variety of effects, including strain induced by the bonding between units that are needed to produce the overall structure, or coordination of some of the oxygen atoms of the rings to cations within the structure. Therefore, the pores in many zeolites are not cylindrical.

The ratio of $Si/Al_2$ determines the hydrophobicity of the adsorbents. Increasing AI content increases the negative charge and this negative charge is balanced by the presence of cations such as $H^+$ or alkali ions like $Na^+$. These charges increase the hydrophilicity of the zeolites. Therefore, a higher Si content is

preferred for the adsorption of hydrophobic molecules. Hydrophobic zeolites are very good adsorbents for hydrocarbons. Hydrocarbons with longer straight chains have higher affinities for zeolites.

The aluminum and silicium atoms are buried in the tetrahedra of oxygen atoms in zeolite frameworks. Therefore, the surface of the zeolite framework is composed of oxygen atoms and this gives zeolites unique adsorption properties. Anionic oxygen atoms are much more accessible by adsorbate molecules and they are more polarizabie than AI and Si cations. Thus, the van der Waals interactions are dominated by anionic oxygen. When zeolite cations are located on the surface, they interact with adsorbate molecules with permanent dipoles. [16]

## 1.5. Aims

The overall aim of this project is to evaluate the feasibility of an adsorption step for the recovery of IA and FA. After carrying out a thorough research in literature it was found out that there were no data for the pairs that can formed by using the following table:

**Table 3: Possible adsorbent – adsorbate pairs**

| Adsorbent | | Adsorbate | | | | |
|---|---|---|---|---|---|---|
| Zeolite | | Chemical Substance (acids) | | | | |
| CBV-28014 | CP 811C-300 | Itaconic | Fumaric | Malic | Citric | Glucose |

Therefore, primary goal of the project is providing experimental data for a certain amount of adsorbent – adsorbate pairs (Table 3) and modelling them, since both IA and FA are promising biochemical building blocks for the future. Sub – objectives of this project are to choose suitable adsorbent, suitable adsorption conditions and to decide which would be the best model to describe the adsorption isotherms.

## 1.6. Outline of the thesis

In an attempt to provide some answers to the questions arisen, adsorption experiments were carried out to estimate the best mathematical model along with its respective parameters to describe the adsorption isotherms. Three different temperatures were chosen to investigate the effect of temperature on equilibrium adsorption and two different zeolites were used to determine the most suitable adsorbent. In this work, it is shown that adsorption using zeolites could be an effective step to increase yield of the downstream process.

## 2. Material and Methods

For the experimental procedure two different zeolites were used, both from Zeolyst International, zeolite CBV-28014 (LOT#: 2200-86) and CP 811C-300 (LOT#: 2200-34). As far as the compounds are concerned, four of them were bought from Sigma Aldrich, IA ≥99% (LOT#: STBC3464V), FA 99% (LOT#: S11357-047), L-(-) - MA (LOT#: 0001409862) and CA (LOT#: 48F - 0109). D (+)-glucose was from Merck KGaA (LOT#: 1.08337.1000). Lab equipment used is stated within the next paragraphs.

**Table 4: Product specifications for the zeolites**

| Adsorbent type | Zeolite type | Pore size (nm) | $SiO_2/Al_2O_3$ mole ratio | Surface area $m^2/g$ |
|---|---|---|---|---|
| **CBV – 28014** | ZSM – 5 (MFI) | ≈ 0.55 | 280 | 400 |
| **CP811C – 300** | BEA | ≈ 0.74 | 360 | 620 |

### 2.1. Initial Experiments

#### 2.1.1. Water evaporation in Greenhouse parallel synthesizer

Initial experiments were carried out to investigate water evaporation in the experimental device. The device used throughout the whole experimental procedure to keep the temperature stable and to magnetically stir the solutions was "Greenhouse parallel synthesizer" from Radley's. The main body of the device is cylindrical and has 4 main components: 1) 24 positions for placing vials, 2) a cooling lid 3) a thermometer to monitor the temperature inside the Greenhouse and 4) a digital screen to adjust temperature (°C) and stirring speed (rpm). Since at later stages aqueous solutions of different components are going to be used at elevated temperatures and samples are going to be taken, it's important to establish reliable results, which essentially means that the concentration of the solutions inside the reaction tubes remain unchanged. For the experiments done pure Milli-Q water was used as the main goal was to test for water mass loss. 5 ml of Milli-Q water were added to 5 reaction tubes and each vial (reaction tube) was placed on a different position inside the greenhouse. Vials were not capped inside the Greenhouse, as evaporation should be prevented by the cooling lid. Temperature inside the Greenhouse was set to 90°C and temperature of the cooling cycle was set to 10°C. The experiment was left to run overnight.

#### 2.1.2. Zeolite Calcination

In addition to experiments mentioned, zeolite powders were calcinated before according to the procedure described by Çagri Efe [16]. Each time a small amount of zeolite(s) was calcinated for further experimental use. The samples were placed in an oven, Carbolite AAF 1100 from Carbolite, for at least 8 hours at 550-600°C and then were stored at 70°C on pre-heated plastic storage vials inside a desiccator to prevent hydration.

## 2.2. Analytical Methods

### 2.2.1. Carboxylic acids with absorption at 210nm

The analysis of the liquid phase was performed using "Thermo Scientific Dionex Ultimate 3000 UHPLC". The experiments carried out were batch experiments and therefore no column was used. This high performance liquid chromatography (HPLC) equipment has an integrated UV – cell and by this way it is possible to analyze the concentration of the eluent, which was being monitored at 210 nm. As a mobile phase Milli-Q water was used at 2 mL/min and the injection volume was 20 μL. The concentrations of the components were determined by constructing a calibration line for each component using the software "Chromeleon" that came with the HPLC equipment.
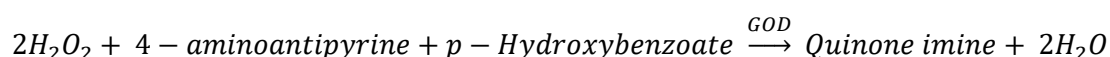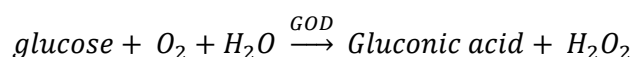
The concentration range investigated for every component was directly defined by the solubility of each one of them to water at 25°C so that the results could be compared (Table 5). Substances such as IA and FA that are solid at room temperature and pressure tend to become more soluble at higher temperatures as it is easier for the solid particles to move between the solution and the solid phase because the kinetic energy increases. This allows the solvent molecules to more effectively break apart the solute molecules that are held together by intermolecular attractions. Therefore, it would be possible to investigate different concentration ranges at different temperatures something that was not done in this work and could be investigated in the future.

Table 5: Solubility and concentration range investigated [3], [Merck Index, 11th Edition]. Solubility was determined from literature in g/L, whereas concentration of experimental solutions was in g/kg

|  | Itaconic acid | Fumaric acid | Malic acid | Citric acid |
|---|---|---|---|---|
| **Solubility in water** | 83g/L @20°C | 4.3 g/L @20°C | 558 g/L @20°C | 750 g/L @20°C |
| **Concentration range investigated** | 0.6046 - 60.46g/kg | 0.05-3g/kg | 25 – 95g/kg | 0.5 - 20g/kg |

### 2.2.2. Glucose

As far as glucose is concerned, since it is a sugar and will not absorb at 210nm (UV spectra), a different method was used to analyze the samples and determine the equilibrium concentration. Megazyme Glucose Reagent is being used. The principle of this method is based on the action of two enzymes, glucose oxidase (GOD) and peroxidase (POD). These two enzymes catalyse the following reactions:

$$glucose + \ O_2 + H_2O \ \xrightarrow{GOD} \ Gluconic \ acid + \ H_2O_2$$

$$2H_2O_2 + \ 4 - aminoantipyrine + p - Hydroxybenzoate \ \xrightarrow{GOD} \ Quinone \ imine + \ 2H_2O$$

In the first reaction hydrogen peroxide is formed during oxidation of glucose by $O_2$ under the influence of glucose oxidase GOD. This $H_2O_2$ is reduced to $H_2O$ under the influence of the enzyme peroxidase, which also creates a red colored compound. Since there is a fixed relationship between the coefficients

of reaction of glucose and of the resulting organic compound, the intensity of red color is a measure of the glucose concentration (colorimetric analysis). The procedure followed is the following:

1. A stock solution is provided containing 1008 mg glucose/1000ml (5600 µmol l$^{-1}$). A calibration sequence is made using this solution by diluting 10, 5 and 2 times with Milli-Q water.
2. The spectrophotometer (LKB novaspec II or V-1200) was turned on at least half an hour before the measurement and after self – calibration wavelength was set to 505nm. Absorbance is set to zero and a water bath is turned on and set at 37ºC.
3. The required number of Eppendorf cups (calibration in triplicate and unknown in duplicate) are put ready
4. Using a pipette, 50 µl of the required solution (calibration or sample) are put in each eppendorf cup.
5. 1ml of glucosereagent is added to all the eppendorf cups and then all the eppendorf cups are mixed well on the vortex.
6. Then the absorption of red color was measured at 505nm.
7. All samples were diluted so that before measuring the concentration of them was below 1 g/L.

## 2.3. Equilibrium time determination

To evaluate the results from the experimental procedure it was necessary to determine the time needed for the system to reach equilibrium at a specific temperature. To measure the equilibrium time, 25ml of stock solution of IA (60.46 g/L) were added to each one of 3 flasks (Table 8). To each one of those flasks a certain amount of CBV-28014 was added. Samples were taken from every flask every 10 minutes and in total 10 samples were obtained from each flask. After sampling, each sample was immediately centrifuged at 32G by using "R11288 Sigma 112" from Sigma-Aldrich to prevent the continuation of the adsorption and establish reliable results. Duration of centrifugation was set to 1min, which was proven to be enough since after that the supernatant liquor was clearly separated from the zeolite.

## 2.4. General Experimental Procedure

After all these preliminary steps were completed, the main experimental work was ready to begin. The experimental procedure followed was the same for every substance (adsorbate):

An initial stock solution was prepared at room temperature the concentration of which was defined (upper limit) by the solubility of the chemical substance at this temperature. The stock solution was produced on a mass basis (g of acid/ kg of solution). The precision of the mass balance was m=10$^{-4}$(g). Afterwards, 10 or 12 solutions of different concentration were prepared and 7g of each were added to 10 or 12 glass vials respectively. After having added the solution, a specific amount of zeolite was added. The added masses of solution and zeolites. When adding the zeolite, the volume $V$ will not remain constant, because of the porosity of the material itself, but in literature it is considered that this small

change of volume does not affect the reliability of the final results and therefore volume *V* was considered to be constant [16]. The adsorption of the acids change the final mass of the solution phase and this mass was not measured. Water loading might generate additional errors in Eq. (8) if not taken into account. However, in previous work done [41], it was showed for CBV 28014 a maximum water loading of 0.039 g/g adsorbent and with the increase in the concentration of a second adsorbate the water loading dropped to values as low as 0.02 g/g adsorbent. These values do not lead to significant errors in the calculations and therefore only the adsorption of acid was taken into account in the loading calculations. Water adsorption was neglected for both zeolites. The glass vials were transferred in the "Greenhouse" where temperature was set to a definite value and continuous stirring was applied (600-1100rpm). Precision of temperature was 1°C and the system was left to equilibrate for at least 2 h and 15 minutes. At 25°C and 50°C evaporation was neglected and a cooling lid was used to prevent losses of liquid (water) to the gas phase. At 70°C, despite preliminary experiments, sealed plastic vials were used instead to ensure that no evaporation would happen. Two samples of 2ml were taken from every vial. The vials were centrifuged to separate the supernatant from the solid phase (zeolite). Centrifugation was performed immediately after sampling to minimize the errors due to temperature shifting and evaporation while handling of the samples. After the separation, each sample was analyzed twice by using the HPLC equipment and exploiting the integrated UV cell. Wavelength was set at 210nm (maximum absorbance wavelength for the 4 acids), flowrate of the mobile phase was 2ml/min, injection volume was 20μl and run time was 1.5min per analysis (3 minutes for 1 samples). The mean value of the measured concentration was taken for every sample. So, by taking a closer look to the mass balance governing the process,

$$q_e = \frac{(C_e - C_o) \cdot V}{m} \qquad (8)$$

, where:

- $q_e$ : amount of adsorbate in the adsorbent at equilibrium (mg/g)
- *Ce*: equilibrium concentration (g/kg)
- *Co*: adsorbate initial concentration (g/kg)
- *V*: volume (ml) or mass of solution (g) of adsorbate
- *m:* mass of the adsorbent (g)

If the adsorbate was measured on a volumetric basis, for example in the early experiments of IA on both zeolites (the equilibrium concentration on these experiments is in g/L instead of g/kg), density (ρ) was used to convert it to a mass basis [42]. By measuring the liquid phase concentration and using the equation mentioned it is possible to calculate the solid phase concentration (g of compound bound to the zeolite/ kg of zeolite).

## 2.5. Statistical Methods

Adsorption has been an effective separation process for a wide variety of applications. Therefore, the consistency and determination of the best fitting model is of utmost importance. One of the major challenges as far as this kind of experiments is concerned is the regression analysis, which basically constitutes the first step towards the statistical analysis.

Regression analysis is a statistical process for estimating relationships among variables. It helps to understand how the value of a dependent variable changes when one independent variable is varied, while the other independent variables are held fixed. The target of this procedure is to estimate the so-called regression function. There are 2 types of regression analysis, linear and non-linear and since many of the adsorption isotherms, which are not linear can be transformed into linear, an explanation as to which one of the 2 forms of the isotherms was preferred is considered to be necessary. The linear regression method approximates that the scatter of points around the line follows a Gaussian distribution and the standard deviation at every value of $C_e$. In reality this behavior is impossible with equilibrium isotherm models. Nonlinear regression method avoids these types of inherent errors making this technique the most appropriate to estimate the isotherm model parameters [43], [44], [45]. Therefore, nonlinear regression analysis was chosen to be applied. The main goal of both linear and non - linear regression analysis (linear is considered to be a special case of nonlinear regression) is the same: Determine the values of the parameters, slope and intercept for linear, or all parameters for non - linear, that, usually, minimize the sum of the squares of the vertical distances of experimental data points from the curve.

### 2.5.1. Parameter Determination

The determination of the best-fit values of the parameters in the model is most of the times the main objective of regression analysis. Side objectives can be the determination of the confidence interval of the estimation of the parameter(s) and the confidence or prediction band of the curve (see 2.5.3). In this work, this has been achieved by using the Gauss–Newton algorithm, which is a method used to solve non-linear least squares problems, integrated in the commercial software Microsoft Office Excel (2010). Non-linear least squares problems arise in non-linear regression, where parameters in a model are sought such that the model is in good agreement with available observations. Statistical methods and isotherm models are interdependent, since model values of the loading ($q_{e, calc}$) are fitted to the experimentally measured loading ($q_{e, exp}$).

### 2.5.2. Error Functions

An error function is the most viable tool used widely to define the best fitting relationship. Their main utility is to quantify the distribution of the adsorbate, provide mathematical analysis of the results and most importantly to verify the consistency of the experimental results, which have led to the generation of the adsorption isotherm. The statistical analysis, in this work, has been completed by evaluating each

adsorption model using 6 different error functions and all of them were calculated by using Microsoft Office Excel (2010). In the following section some new parameters/symbols are introduced:

- ✓ $q_{e,calc}$ is the equilibrium capacity calculated from the model
- ✓ $q_{e,exp}$ is the experimentally measured loading
- ✓ $y_i$ is the dependent observed variable
- ✓ $y_{calc}$ is the dependent variable calculated by the model and
- ✓ $\bar{y}$ is the mean value of $y_i$
- ✓ $n$ is the number of data points
- ✓ $p$ is the number of parameters fit
- ✓ $SSE$ is the sum of squared errors
- ✓ $SST$ is the sum of squared totals

- **Sum square error (ERRSQ)**

It is probably the most used error function. It has one drawback, it will provide a better fit at the higher concentration range due to the fact that the magnitude of the errors and as a result the square of the errors will increase as concentration increases.

The equivalent mathematical statement is:

$$ERRSQ = \sum_{i=1}^{n} \left(q_{e,calc} - q_{e,exp}\right)_i^2 \qquad (9)$$

- **Hybrid fractional error function (HYBRID)**

This error function was developed to improve the fit of the *ERRSQ* method at low concentration values. In this method, each *ERRSQ* value was divided by the experimental solid phase concentration q value. In addition, a divisor was included as a term for the number of degrees of freedom for the system, the number of data points minus the number of parameters within the isotherm equation. The equivalent mathematical statement is:

$$HYBRID = \frac{100}{n-p} \sum_{i=1}^{n} \left[ \frac{\left(q_{e,calc} - q_{e,exp}\right)^2}{q_{e,exp}} \right]_i \qquad (10)$$

- **Average relative error (ARE)**

*ARE* is an indication about the tendency to under or overestimate experimental results throughout the whole concentration area. The equivalent mathematical statement is:

$$ARE = \frac{100}{n-p} \sum_{i=1}^{n} \left| \frac{q_{e,calc} - q_{e,exp}}{q_{e,exp}} \right|_i \qquad (11)$$

- **Marquardt's percent standard deviation (MPSD)**

Marquardt's percent standard deviation (MPSD) error is similar to some aspects of a modified geometric mean error distribution according to the number of degrees of freedom in the system.

The equivalent mathematical statement is:

$$MPSD = 100 \left( \sqrt{\left( \frac{1}{n-p} \sum_{i=1}^{n} \left[ \frac{\left(q_{e,calc} - q_{e,meas}\right)^2}{q_{e,meas}} \right] \right)} \right) \qquad (12)$$

- **Adjusted coefficient of determination ($R^2$)**

The $R^2$ quantifies the goodness of the fit and it is a unitless fraction between 0 and 1. Higher values indicate that the model fits the data better. It has to be pointed out, though, that there is no general rule about what values of $R^2$ are high, adequate or low and due to this it is not correct to overemphasize on the value of $R^2$. A higher value indicates that the curve is very close the experimental points and that does not necessarily mean that the fit is generally "good". As a result, a look at a combination of factors (results, error functions) is needed for a solid determination of the "best-fit".

In addition to this, when comparing models, usually the more the parameters the better the estimation, so the one with more parameters can bend more to come closer to the experimental points resulting in better fit. The adjusted $R^2$ takes into account the number of the parameters of every model so that the comparison between models with different numbers of parameters is feasible. The adjusted $R^2$ is smaller than the ordinary $R^2$, whenever the number of parameters *(p)* is greater than 1.

The equivalent mathematical statement is:

$$R^2 = 1 - \frac{SSE}{SST} \tag{13}$$

$$Adjusted\ R^2 = 1 - \frac{SSE/(n-p)}{SST/(n-1)} \tag{14}$$

, where

$$SSE = \sum_{i=1}^{n} (y_i - y_{calc})^2 \tag{15}$$

$$SST = \sum_{i=1}^{n} (y_i - \bar{y})^2 \tag{16}$$

- **Nonlinear chi-square test ($\chi^2$)**

Nonlinear chi-square test is a statistical tool used to find the best fit of an adsorption system and it is obtained by evaluating the sum the sum squares differences between the experimental and the calculated data, with each squared difference is divided by its corresponding value (calculated). The smaller the value of $\chi^2$ is, the more the similarities are and vice versa. The advantage of using chi-square test is comparing all isotherms on the same abscissa and ordinate.

The equivalent mathematical statement is:

$$\chi^2 = \sum_{i=1}^{n} \frac{(q_{e,exp} - q_{e,calc})^2}{q_{e,calc}} \tag{17}$$

### 2.5.3. Reliability of the results

Of course one of the main question arisen is the reliability of the results, because the error functions are only able to provide absolute numerical data (sums) that can be compared for every adsorption isotherm (model). What they are not able to specify is the trustworthiness (reliability) of the results. To do so, two new terms are introduced:

**Confidence Interval – Band**

Most of the times the entire goal of nonlinear regression is to compute the best-fit values of the parameters in the model. A 95% confidence band encloses the area in which someone can be 95% sure that the true curve is contained. The most useful advantage is the visual sense of how well experimental data define the best-fit curve. Wide confident intervals mean that data used do not define the parameter very well. The determination of confidence intervals is a result of the standard errors of the parameters. By determining the confidence intervals someone can estimate how "tightly" these values have been calculated.

## Prediction Interval – Band

Confidence intervals are closing related to prediction intervals and a 95% prediction band encloses the area that someone expects to enclose 95% of future data points. One major advantage of the prediction interval is that it already includes both the uncertainty concerning the true position of the curve (confidence band) and also accounts for an issue often concerning experimentalists, the scattering of the data around the curve. Therefore, someone can easily understand why a prediction band is always wider than a confidence band.

It has to be pointed out that intervals and bands are closely related one to another. Confidence intervals represent the uncertainty in an estimate of single numerical value, whereas a confident band is used in statistical analysis to represent the uncertainty in an estimate of a curve or function based on limited and/or noisy data. Similarly, a prediction band is used to depict the uncertainty related to the value of a new data – point on the curve, but subject to noise. As made clear, bands are usually used as part of the graphical presentation of results of a regression analysis. In addition to this, the following points are mentioned, because sometimes

- A 95% confidence interval does not mean that 95% of the sample data lie within the interval.

- A confidence interval is not a range of plausible values for the sample mean, though it may be understood as an estimate of plausible values for the population parameter.

- A particular confidence interval of 95% calculated from an experiment does not mean that there is a 95% probability of a sample mean from a repeat of the experiment falling within this interval. [46]

Notice: Confidence intervals of the parameters as well as confidence and prediction bands shown in figures have been calculated using commercial software [47]. Mathematical background and formulas – equations concerning the confidence intervals and bands are not mentioned. All of these can be found in Help -> Methods and Formulas of *Minitab*

### 2.5.4. Choosing the best – fit model

Apart from all these, it should also be taken into consideration that the statistical analysis of the results is the most important step before evaluation results and drawing conclusions.

Due to scattering and deviations of the experimental data, sometimes on the same zeolite – compound pair a different isotherm model seems to fit better at different temperatures. As a result, a credible final conclusion is not always an easy case or sometimes the choice of the isotherm is based on the personal perspective of evaluating the error functions. Therefore, the analysis of the work done is made based on the assumption that the mechanism of a certain adsorbent – adsorbate pair does not change with shifts in temperature and the best – fitting model is determined by calculating the average value of every error function for every possible model for each zeolite – compound pair. The average value is derived by the experimental data at the different temperatures investigated. This way, the choice of a single isotherm is not only simplified, but also more credible.

As a consequence, a careful selection and utilization of the evaluation tools is necessary. Based on the experimental results and after completing the analysis is completed, the criteria (Error Functions) with the aid of which the best – fitting model is chosen as well as why these criteria were chosen e.g. faceted evaluation of the results and enhanced reliability should be clear.

# 3. Results and Discussion

## 3.1. Water Evaporation

Results from water evaporation experiments can be seen in the following table. Water mass was measured before and after.

**Table 6: Experimental data for water evaporation after heating to 90ºC and cooling back to 30ºC**

| | | Before | After | Difference | |
|---|---|---|---|---|---|
| **Vial ID** | Vial+Water (g) | Water mass (g) | Water mass (g) | Change (%) | Greenhouse position |
| 1 | 17.896 | 5.008 | 4.970 | -0.751 | A4 |
| 2 | 17.845 | 5.022 | 4.991 | -0.617 | B3 |
| 3 | 17.916 | 5.024 | 4.984 | **-0.810** | C2 |
| 4 | 17.941 | 5.023 | 4.996 | -0.544 | D6 |
| 5 | 17.985 | 5.029 | 4.994 | -0.694 | E5 |

Vials were heated up to 90ºC and then cooled back to 30ºC. No significant water evaporation was observed and therefore loss of water mass is negligible (max value highlighted). Mass loss was not affected by the position of the vial in the "Greenhouse" and as a consequence it is possible to further proceed with experiments using the device, because the highest temperature at which they were going to be performed was 20ºC degree lower than the temperature of this test.

## 3.2. Zeolite Calcination

Mass before and after calcination were measured and mass change was calculated for both zeolites and the results can be seen in Table 7. For the calcination samples, it can be observed that mass change was significantly larger for CP811C – 300 (-12.37 %) in comparison to the respective one for CBV – 28014 (-2.41 %). Therefore, zeolite calcination is a crucial step before using zeolites, which, if omitted, will generate additional errors to the modelling. More results can be seen in Table A. 1, Table A. 2 and Table A. 3

**Table 7: Mass loss of zeolites after calcination**

| | Before Calcination | After Calcination | Difference |
|---|---|---|---|
| **Zeolite** | Amount of Zeolite(g) | Amount of Zeolite (g) | Change (%) |
| **CBV-28014** | 10.07 | 9.83 | -2.41 |
| **CP811C-300** | 10.00 | 8.40 | -12.37 |

## 3.3. Equilibrium Time

Time needed for the system to reach equilibrium was investigated. In the following table (Table 8) the amount of zeolite and mass of solution added can be seen:

Table 8: Equilibrium experiment

|  | Flask 1 | Flask 2 | Flask 3 |
| --- | --- | --- | --- |
| Empty mass (g) | 56.569 | 54.023 | 55.796 |
| Zeolite added (g) | 1.799 | 1.871 | 1.779 |
| Total flask mass (g) | 58.367 | 55.893 | 57.575 |
| Mass of solution (g) | 25.300 | 25.625 | 25.590 |

In the following Figure 10, equilibrium adsorption is plotted against time.
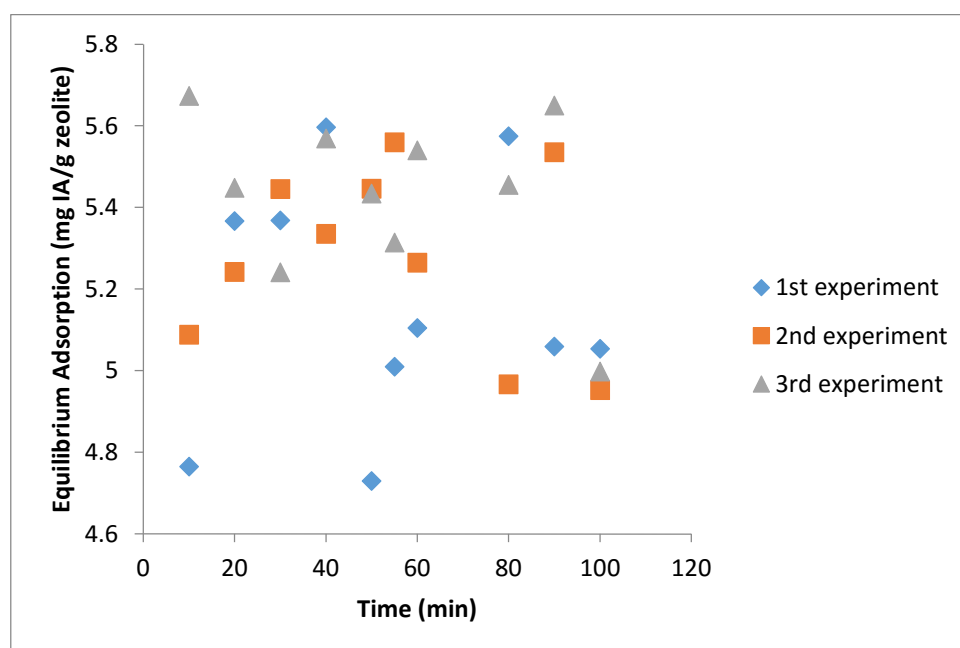


Figure 10: Determination of equilibrium time

Although a clear trend towards a constant concentration is not visible, 135 minutes were thought to be sufficient for the system to equilibrate, as no further increase in equilibrium adsorption seems to be happening after 80 minutes. Based on the equilibrium time for IA, every component was left to equilibrate for at least 2 h and 15 minutes at all temperatures.

## 3.4. Isotherms

Experimental points that showed negative equilibrium adsorption have been deleted. In addition to this, experimental points that were outside the prediction band have been omitted and the analysis has been rerun once. The choice of the best – fitting model is the most difficult and complex part of this work.

This is the reason for which every model was evaluated using 5 different error functions (see Eq. 10, 11, 12, 14, 17). A summarizing table of all these error functions was created for every pair of adsorbent – adsorbate over 3 different temperatures (see Choosing the best – fit model) and the average values were calculated (Table 9 and Table A. 4 - Table A. 10). Since there is not a single error function that combines the ones mentioned into one, a separate examination of each result of the error estimation methods is necessary. In that context, it has to be mentioned that all the error functions (except for $\chi^2$) include a term in their mathematical expression that takes into account the number of the inner parameters of every model and therefore comparison of the results shown in Table 9 between models that do not contain the same number of parameters is feasible. In Table 9, adjusted $R^2$ of Sips is higher, HYBRYID, MPSD and ARE of Sips are significantly lower and Chi – square of Sips is extremely larger. If the choice was based only on Chi – square, then Redlich – Peterson would be the best fitting model, but after applying an overall comparative evaluation between all the error estimation methods Sips isotherm was chosen. In Table 10, the values of the error functions of Sips are all better compared to the rest of the models and therefore the choice of Sips is evident. The evaluation of all these error estimation methods showed that the Sips model provides the best fit for the experimental equilibrium data over 3 temperatures for almost every pair of adsorbent – adsorbate. Only in the case of CA, single Langmuir provided better fits, but due to the limited number of experimental points, concentration range and low correlation (especially on zeolite CBV – 28014 Table A. 9), more experiments should be done.

In Figure 11, experimental data along with the fitted Sips adsorption model, prediction and confidence intervals can be seen. Fitted parameters are shown in Table 11. Experimental data seem to be fitting very well and as a result confidence and prediction bands are pretty narrow. In contradiction to this, in Figure A. 5, scattering is greater and therefore the bands are wider. There are also cases, where scattering is even greater, just like in Figure A. 18, where confidence band is even wider. The rest of the isotherms along with their parameter estimation can be found in the Appendix section: Adsorption Isotherms. In the next figures only fitted curves will be presented given the large number of experiments and experimental points.

**Table 9: Summarizing table of error functions for IA on CBV - 28014 over 3 different temperatures – Average values (highlighted values are better i.e. highest adjusted R2 and lowest ARE, MSPED, HYBRID, $\chi^2$)**

|  | Freundlich | Single Langmuir | Double Langmuir | Sips | Toth | Redlich - Peterson |
|---|---|---|---|---|---|---|
| **Adjusted $R^2$** | 0.7472 | 0.8652 | 0.8534 | **0.9450** | 0.8596 | 0.9163 |
| **Chi-square $\chi^2$** | 200.93 | 118.80 | 118.80 | 8654.26 | 118.80 | **96.98** |
| **HYBRYID** | 11952.95 | 5708.21 | 6484.42 | **232.84** | 6070.41 | 3690.15 |
| **MPSD** | 956.64 | 661.26 | 699.68 | **134.27** | 679.58 | 524.38 |
| **ARE** | 2776.25 | 1719.34 | 1978.23 | **30.41** | 1839.66 | 1423.91 |

**Table 10: Summarizing table of error functions for FA on CP811C - 300 over 3 different temperatures – Average values (highlighted values are better i.e. highest adjusted R2 and lowest ARE, MSPED, HYBRID, $\chi^2$)**

|  | Freundlich | Single Langmuir | Double Langmuir | Sips | Toth | Redlich - Peterson |
|---|---|---|---|---|---|---|
| **Adjusted R2** | 0.9263 | 0.9519 | 0.9504 | **0.9586** | 0.6860 | 0.6806 |
| **Chi-square χ2** | 39.29 | 20.84 | 16.94 | **15.56** | 34.58 | 31.96 |
| **HYBRYID** | 1092.06 | 421.90 | 348.64 | **121.07** | 1134.63 | 1164.25 |
| **MPSD** | 262.93 | 175.95 | 166.02 | **108.89** | 301.38 | 305.51 |
| **ARE** | 112.62 | 72.89 | 71.35 | **40.74** | 133.01 | 133.78 |



**Figure 11: Adsorption of IA on CBV – 28014 at 50°C**

**Table 11: Sips parameter estimation for IA on CBV – 28014 at 50°C**

| Parameter | Estimate | Standard Error | 95% Confidence Interval | |
|---|---|---|---|---|
|  |  |  | **Lower** | **Upper** |
| **Ks** | $5.555 \cdot 10^{-2}$ | $6.49 \cdot 10^{-2}$ | $1.91 \cdot 10^{-3}$ | $4.749 \cdot 10^{-1}$ |
| **βs** | 4.228 | $6.422 \cdot 10^{-1}$ | 3.047 | - |
| **αs** | $5.772 \cdot 10^{-4}$ | $7 \cdot 10^{-4}$ | - | - |

In the following Figure 12, Figure 13, Figure 14, Figure 15, four comparative charts are presented depicting the relation between the four different compounds and zeolite CBV – 28014 at three different temperatures. Equilibrium adsorption is higher at lower temperatures confirming the initial guess about the effect of temperature. Apart from this, temperature affects the adsorption of every compound in a

different way: Sometimes there is a large drop during the first increase of temperature (Figure 13), sometimes there is a significant drop when increasing from 50 to 70ºC such as in Figure 12. In Figure 14 the drop is more or less the same during the 1st and the 2nd increase of temperature. Similar conclusion related to zeolite CP811C-300 can be drawn by looking at Figure A. 23 - Figure A. 26.
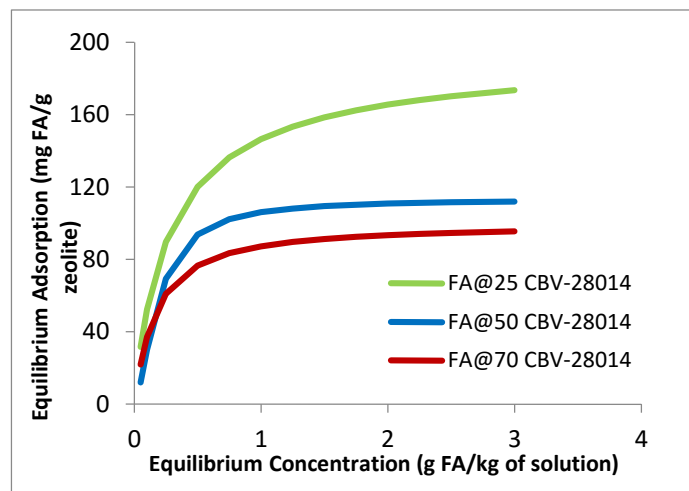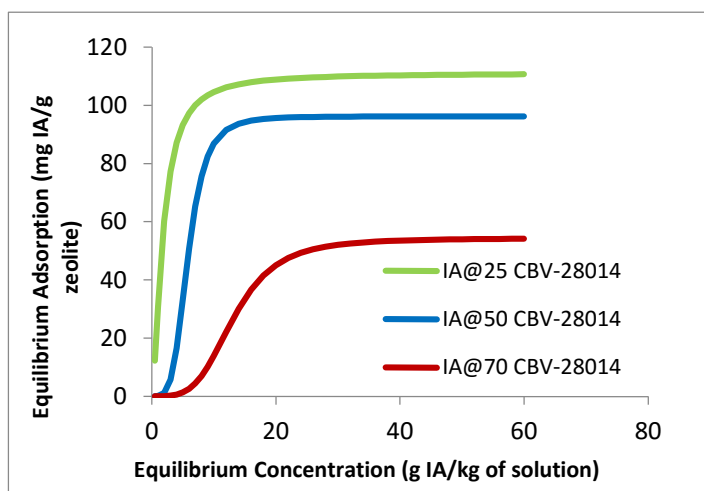


**Figure 12 (left): IA adsorption on CBV-28014 at 3 different temperatures and Figure 13 (right): FA Adsorption on CBV-28014 at 3 different temperatures**
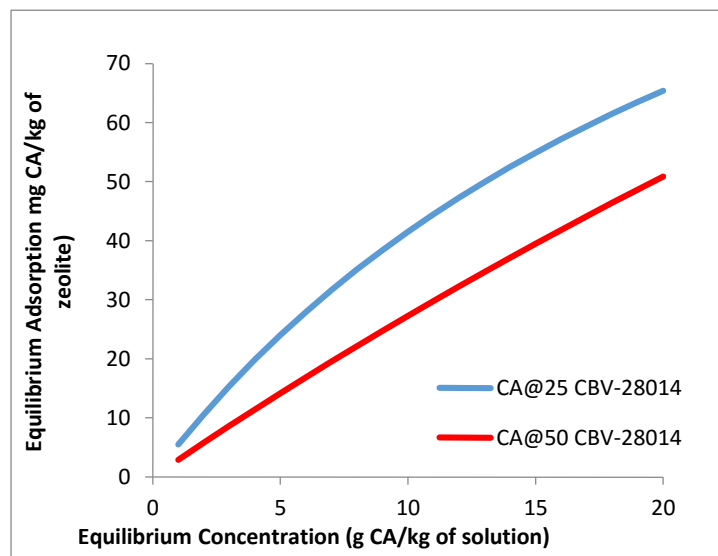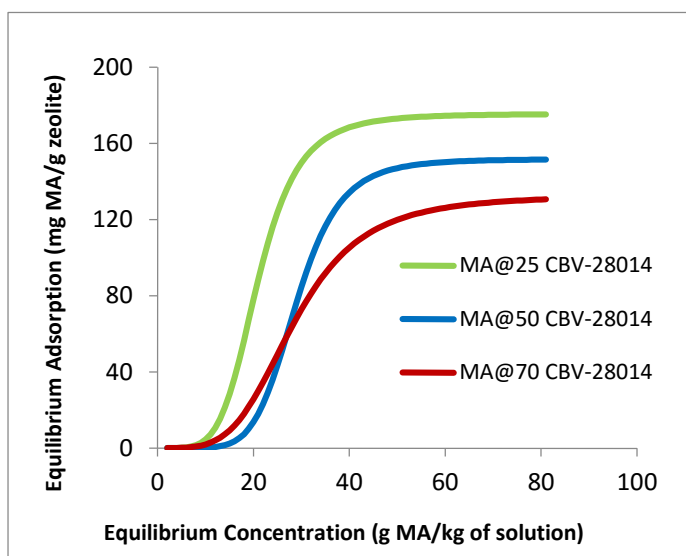


**Figure 14 (left): MA Adsorption on CBV-28014 at 3 different temperatures and Figure 15 (right): CA Adsorption on CBV-28014 at 2 different temperatures**

| Parameter | IA | | | FA | | | MA | | |
|---|---|---|---|---|---|---|---|---|---|
| | 25°C | 50°C | 70°C | 25°C | 50°C | 70°C | 25°C | 50°C | 70°C |
| Ks | 42.56 | $5.555 \cdot 10^{-2}$ | $2.720 \cdot 10^{-3}$ | 598.7 | 1654 | 695.2 | $9.565 \cdot 10^{-6}$ | $9.853 \cdot 10^{-8}$ | $9.422 \cdot 10^{-6}$ |
| βs | 1.626 | 4.228 | 3.834 | 0.921 | 1.607 | 1.071 | 5.5 | 6.287 | 4.914 |
| αs | 0.383 | $5.772 \cdot 10^{-4}$ | $5.010 \cdot 10^{-5}$ | 3.088 | 14.60 | 6.969 | $5.531 \cdot 10^{-8}$ | $6.496 \cdot 10^{-10}$ | $7.413 \cdot 10^{-8}$ |

Table 13: Parameters of single Langmuir for CA on CBV-28014 at 2 different temperatures

| Parameter | Estimate | |
|---|---|---|
| | 25°C | 50°C |
| qsat | 153.6 | 373.3 |
| $k_L$ | $3.708 \cdot 10^{-8}$ | $7.886 \cdot 10^{-3}$ |

In the following Figures (Figure 16, Figure 17, Figure 18), the isotherms of IA, FA and MA on zeolite CP811C – 300 at a single temperature can be observed. Apart from the strong adsorption of IA and FA in the lowest concentrations, especially at 25°C and 50°C, it is also visible that at 25°C MA shows the largest binding capacity (when concentration is > 30 g/kg), whereas at 50 and 70°C IA is the compound with the highest value. Increase in temperature is not favorable for MA and IA has a more stable performance on this zeolite. Similar conclusion concerning zeolite CBV – 28014 can be drawn by looking at Figure A. 27, Figure A. 28.
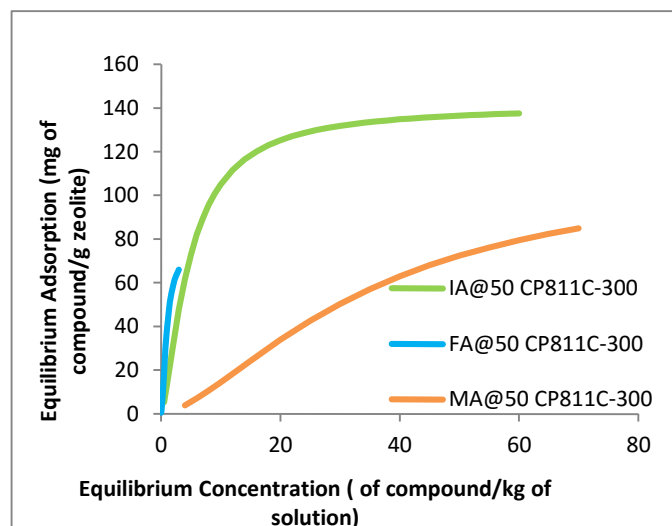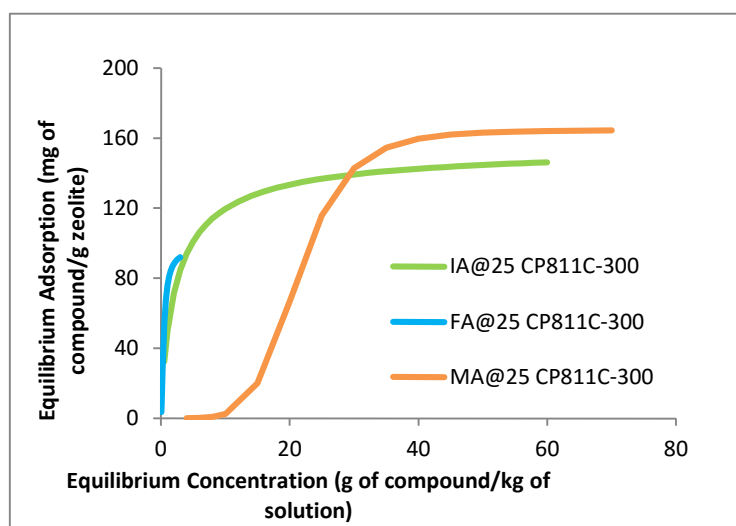


Figure 16 (left): Adsorption of compounds at 25 °C on CP811C-300 and Figure 17 (right): Adsorption of compounds at 50°C on CP811C-300
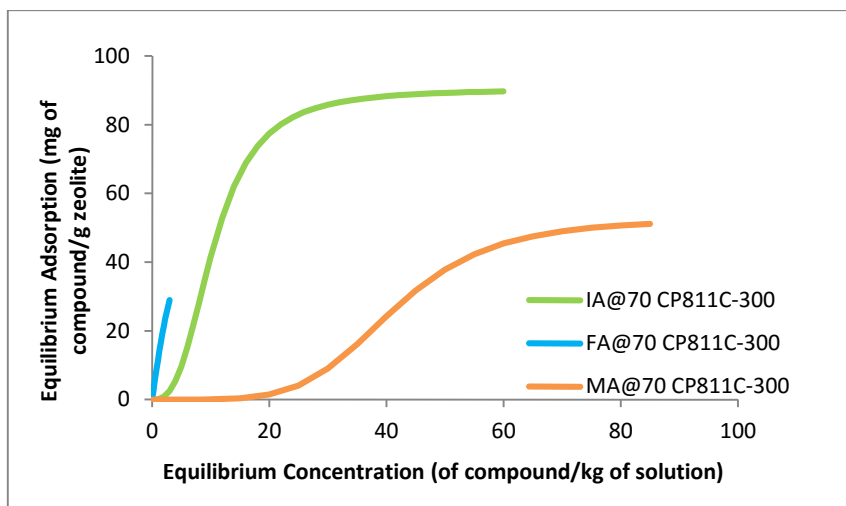
Table 14: Sips parameter estimation IA, FA and MA at 25 ºC, 50 ºC and 70 ºC on CP811C-300

| Parameter | 25ºC | | | 50ºC | | | 70ºC | | |
|---|---|---|---|---|---|---|---|---|---|
| | IA | FA | MA | IA | FA | MA | IA | FA | MA |
| Ks | 73.21 | 348.6 | $2.256 \cdot 10^{-7}$ | 14.83 | 80.13 | 0.4680 | 0.1156 | 13.64 | $5.7 \cdot 10^{-7}$ |
| βs | 0.8453 | 1.532 | 6.678 | 1.440 | 1.682 | 1.547 | 2.821 | 1.131 | 4.930 |
| αs | 0.4695 | 3.606 | $1.407 \cdot 10^{-9}$ | 0.1051 | 1.058 | 0.0041 | 0.00128 | 0.1818 | $1.085 \cdot 10^{-8}$ |

### 3.4.1. Effect of temperature

First of all, by checking Figure 12 - Figure 15 it can be observed that, generally, the adsorption process is favored at lower temperatures as expected since most of the adsorption processes are exothermic and therefore with an increase in temperature, adsorption decreases [48]. Specifically, all of the compounds are adsorbed stronger at 25ºC and less strong at 50ºC. At 70ºC the adsorbance is weaker and sometimes it drops significantly, but sometimes the drop can occur at 50ºC. In addition to this, sometimes in low concentrations, adsorption is stronger at a higher temperature (Figure 13, Figure 14) and it should be further investigated.

### 3.4.2. Effect of zeolite

Both zeolites seem to be performing well enough, but of course there are trends between the 2 different zeolites. For IA, the performance of both zeolites is similar. At 25ºC and 50ºC, there is strong adsorption of IA in the low concentrations, something that decreases if the temperature is increased at 70ºC. In addition to this, the change in adsorption during the 1st increase of temperature is more or less the same

for both zeolites, but on the 2$^{nd}$ increase CP811C-300 seems to be performing better compared to CBV-28014 (large drop). As far as FA is concerned, the effect of zeolite in this case is stronger and the trend is not exactly the same. On CBV-28014, by increasing from 25$^{o}$C to 50$^{o}$C, there is a huge drop in equilibrium adsorption, but if the temperature is further increased the drop is smaller. On CP811C-300, drops in adsorption with increasing temperature are smoother. For MA, on CBV-28014, increasing the temperature from 25$^{o}$C to 50$^{o}$C and then to 70$^{o}$C will result to small drops in adsorption on every stage, whereas on CP811C-300 there is a huge drop on the 1$^{st}$ increase in temperature and a smaller one on the 2$^{nd}$ increase. Finally, for CA, on CP811C-300, the drop in adsorption if the temperature is increased from 25$^{o}$C to 50$^{o}$C is larger compared to the drop for the same increase on CBV-28014.

### 3.4.3.  Effect of compound (sorbate – sorbent)

Based on the analysis done before, adsorption is higher at lower temperatures on both zeolites and different trends may apply. Of course something that cannot be ignored is that when investigating a different pair of sorbate – sorbent, different trends may also apply, because every sorbent (zeolite) is natural to perform differently if the sorbate (compound) changes. For example, on CP811C-300 (Figure 16, Figure 17, Figure 18), on low concentrations adsorption of FA is strong, stronger than adsorption of itaconic or MA. In the range of 10-50g/kg, itaconic and malic adsorb more and at different temperatures different correlations exist, at 25$^{o}$C adsorption of malic is higher, whereas at 50 or 70$^{o}$C adsorption of IA is higher. For FA some restrictions apply due to its solubility and therefore a comparison is not always possible. In addition to this, adsorption of MA in the same concentration range is pretty low and sometimes close to zero and of course this is something to be investigated (the shape of the curve), but it is more than clear that CP811C-300 behaves differently on different compounds. As far as CBV-28014 is concerned, by taking a closer look at Figure A. 27, Figure A. 28 and Figure A. 29 someone can observe that trends are not the same. Of course there is strong adsorption of fumaric and IA at low concentrations and weak adsorption of malic on the same range, but at higher concentrations MA adsorption is always higher than IA adsorption. Therefore, not only performance of these 2 different zeolites is not the same on these 3 compounds, but also their behavior is different.

### 3.4.4.  Effect of pH

pH was not measured during the experiments carried out. Low pH could explain the low adsorption at low concentrations, which resulted to S – shaped adsorption isotherms. The reason is that at low pH the acids will dissociate and therefore less non-dissociated acid (less chemical compound to be adsorbed, see 1.2.1) will be present resulting to nearly to zero equilibrium adsorptions. Sips model seems to be doing better at higher concentrations and therefore further investigation is required in the lowest concentrations

## 3.5.    Citric acid and glucose

Adsorption results of CA are not included in the comparative charts due to the fact that correlation was not high enough (Table A. 9) and the concentration range investigated was not very broad (0 – 20 g/kg). Some additional experiments of glucose adsorption have been done. In Figure 19 and Figure 20 experimental results are shown. Based on this data, glucose adsorption is very low on both zeolites and more precisely negative values of binding capacity might indicate higher affinity towards water adsorption instead of glucose, which may be too big for the pores of the zeolites. Due to these results, experiments were done only at 25°C. A 2nd batch of experiments has been carried out to confirm (Figure A. 30 - Figure A. 31) resulting to the same conclusion.
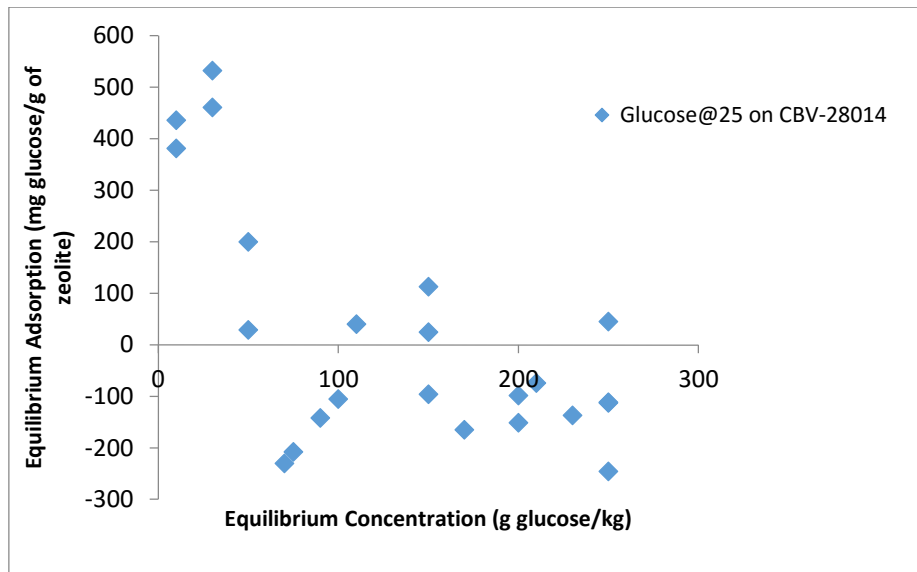


**Figure 19: Glucose adsorption at 25 °C on CBV-28014**
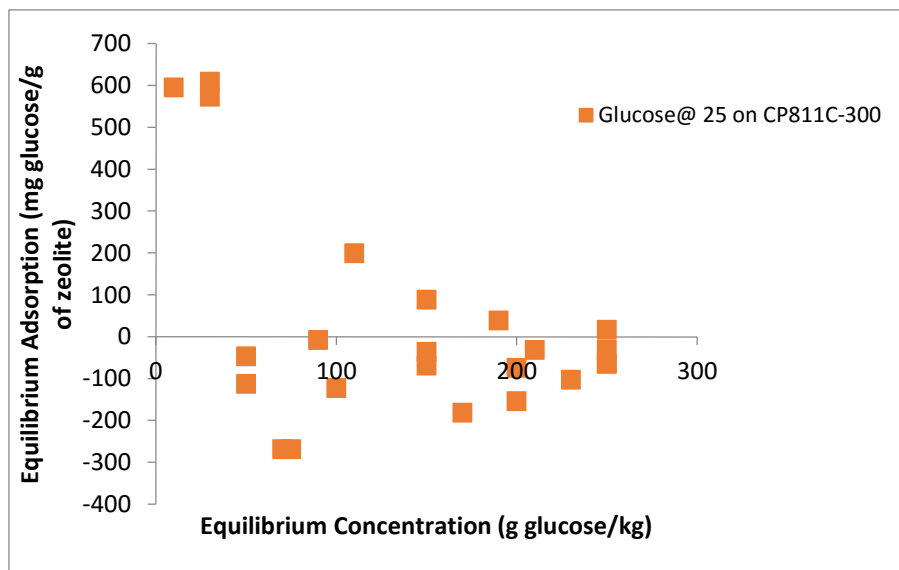


**Figure 20: Glucose adsorption at 25 °C on CP811C-300**

33

All of the above effects are reflected collectively in Figure 21 - Figure 24
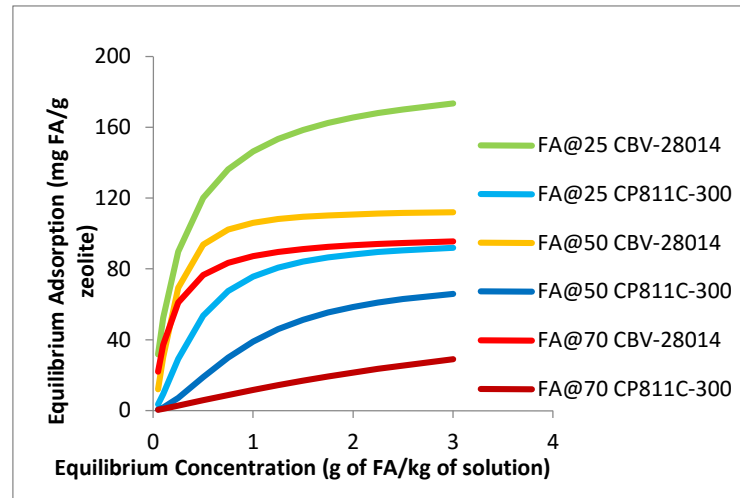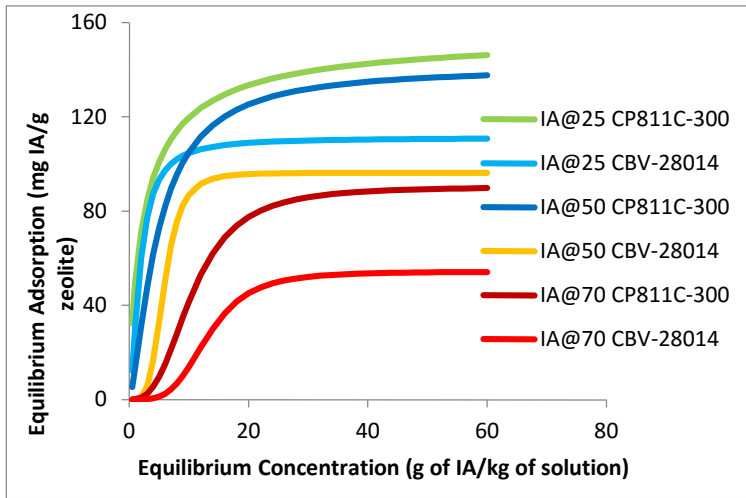


**Figure 21 (left): Adsorption of IA on 2 different zeolites at 3 different temperatures and Figure 22 (right): Adsorption of FA on 2 different zeolites at 3 different temperatures**
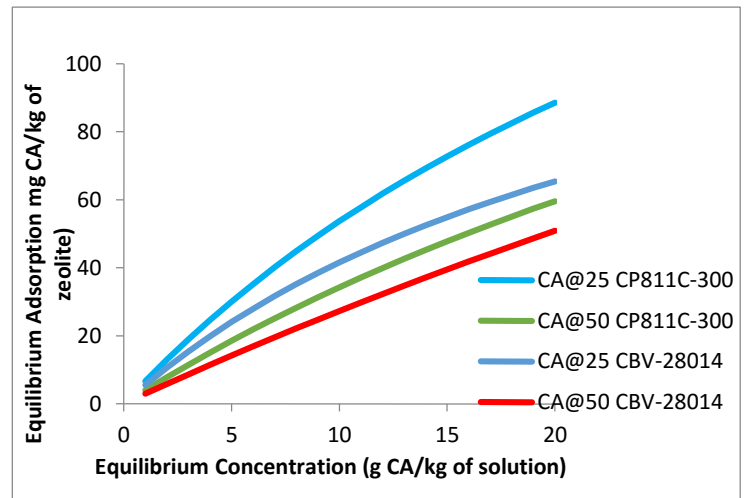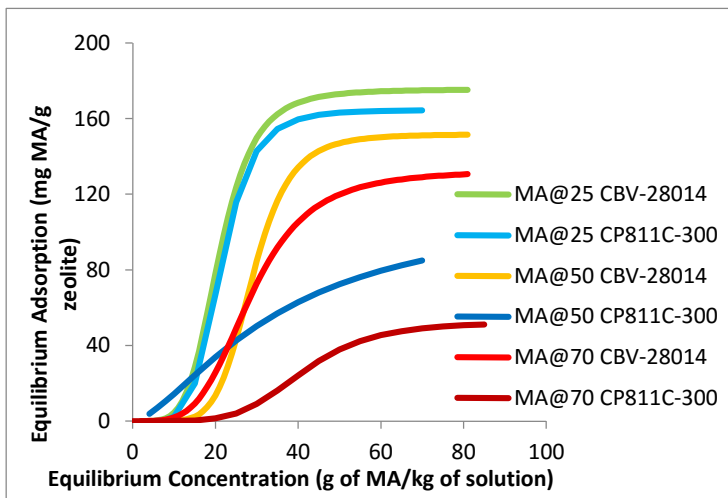


**Figure 23 (left): Adsorption of MA on 2 different zeolites at 3 different temperatures and Figure 24 (right): Adsorption of CA on 2 different zeolites at 2 different temperatures**

# 4. Conclusions

Adsorption of IA, FA, MA, and glucose on two different zeolites (CP811C-300 & CBV-28014) was measured. The measured loading at different concentrations at 3 different temperatures showed that zeolite loadings of each compounds are higher at lower temperatures. This indicates that adsorption of the four investigated compounds is exothermic. Furthermore, adsorption is particularly strong for IA and FA at low concentrations compared to the other two compounds. Glucose is barely adsorbed at any of the investigated temperature and concentrations.

The statistical analysis performed on the established data by fitting it to 6 different isotherms models, and the fits were evaluated using 5 error functions. The results indicate that the Sips model is the models with the best fit to the experimental data. However, CA should be retested because the results were not conclusive.

The current results indicate that the use of CP811C – 300 in IA recovery and the use of CBV – 28014 in FA recovery might be an efficient option, but additional studies will be also required with respect to the affinities of the 2 zeolites towards MA and CA. Since real fermentation broths will contain also impurities, the IA and FA loadings will be different. However, the competitive effect of the impurities might be insignificant due to their expected lower concentrations. It would be interesting if adsorption batch experiments with mixed solutions had been performed in this study to investigate the effect of the impurities. Therefore, an overall evaluation of the overall process is required.

# 5. Recommendations for the future

Some recommendations for future work are listed below:

- Investigate the adsorption of these compounds at higher temperatures or at either more broad concentration ranges or higher concentrations (closer to the solubility). Closer investigate specific concentration ranges for every compound: IA 0 – 10 g/kg, FA 2.5 – 4 g/kg, MA 0 – 20 g/kg

- Investigate the adsorption of these compounds on other zeolites or other materials (activated carbon)

- Due to the shape of some curves at low concentrations (extremely small values of the parameters), some of the experiments should be repeated by using an equipment that will behave better at this range. Some of the inaccuracy is due to the inherent errors of the equipment. A UHPLC with a different UV – Cell (longer path length) could be used instead to increase accuracy.

- All of the experiments or future experiments could be repeated by using an auto-sampler to decrease experimental time, increase injection accuracy and produce a higher amount of experimental results.

- The experiments performed were single compound batch experiments. In order for the results to be fully exploitable and investigate scale – up for potential industrial applications, multicomponent mixtures should be tested by carrying out either batch or column experiments, which will give a much better understanding of the overall adsorption process. A typical fermentation broth contains several chemical compounds and it would be extremely useful to understand and estimate the interaction between them.

# 6. Acknowledgements

First and the foremost, I would like to offer my sincere gratitude to my master thesis daily supervisor, Erik Häusler, PhD candidate at TU Delft, for his enthusiasm on the project and for his being consistently available whenever I needed him. His scientific knowledge and his supportive attitude were catalytic in the completion of my project as I always found his helping hand. I am also thankful to the support staff of the Bioprocess Engineering Department for their constant help whenever I needed it. I would like to extend my sincere thanks to my friends and colleagues, who supported me and I wish to profoundly acknowledge the contribution of my professor at my home university, Antonis Kokossis, who unconditionally supported and promoted me as an exchange student. Last but not the least, I would like to express my warmest thanks and gratitude to Dr.ir. A.J.J. (Adrie) Straathof for accepting my application and trusting me.

# 7. Nomenclature

$q_e$: amount of adsorbate in the adsorbent at equilibrium (mg/g)

$K_F$: Freundlich isotherm constant (mg/g) $(kg/g)^n$ related to adsorption capacity

$n$: adsorption intensity

$q_{sat}$ or $q_{max}$: maximum monolayer coverage capacities (mg/g)

$k_L$: Langmuir isotherm constant (kg/g)

$a_S$: Sips isotherm model constant (kg/g)

$K_S$: Sips isotherm model constant (g/g)

$\beta_S$: Sips isotherm model exponent

$a_T$: Toth isotherm constant (g/kg)

$K_T$: Toth isotherm constant (g/g)

$t$: Toth isotherm constant

$a_R$: Redlich–Peterson isotherm constant (kg/g)

$K_R$: Redlich–Peterson isotherm constant (g/g)

$g$: Redlich - Peterson isotherm exponent

$Ce$: equilibrium concentration (g/kg)

$Co$: adsorbate initial concentration (g/kg)

$y_i$ : dependent observed variable

$y_{calc}$ : dependent variable calculated by the model and

$\bar{y}$: mean value of $y_i$

$n$: the number of data points

$p$: number of parameters fit

$V$: volume (ml) or mass of solution (g) of adsorbate

$m$: mass of the adsorbent (g)

$q_{e,calc}$: equilibrium capacity calculated from the model (mg/g)

$q_{e,exp}$: is the equilibrium capacity (mg/g) calculated from the experimental data

$SSE$: Sum of squared errors

$SST$: Sum of squared totals

$\chi^2$: Nonlinear chi-square test

$HYBRID$: Hybrid fractional error function

$ARE$: Average relative error

$MPSD$: Marquardt's percent standard deviation

$ERRSQ$: Sum square error

$R^2$: Adjusted coefficient of determination

# 8. Appendix

**Table A. 1: Mass loss of zeolites after calcination**

|  | Before Calcination | After Calcination | Difference |
|---|---|---|---|
| **Zeolite** | Amount of Zeolite(g) | Amount of Zeolite (g) | Change (%) |
| **CBV-28014** | 19.81 | 19.35 | -2.32 |
| **CP 811C-300** | 16.84 | 16.38 | -2.73 |

**Table A. 2: Mass loss of zeolites after calcination**

|  | Before Calcination | After Calcination | Difference |
|---|---|---|---|
| **Zeolite** | Amount of Zeolite(g) | Amount of Zeolite (g) | Change (%) |
| **CBV-28014** | 12.51 | 12.22 | -2.32 |
| **CP 811C-300** | 12.91 | 10.85 | -15.96 |

**Table A. 3: Mass loss of zeolites after calcination**

|  | Before Calcination | After Calcination | Difference |
|---|---|---|---|
| **Zeolite** | Amount of Zeolite(g) | Amount of Zeolite (g) | Change (%) |
| **CBV-28014** | 18.32 | 17.80 | -2.96 |
| **CP 811C-300** | 14.50 | 12.20 | -15.39 |

**Table A. 4: Summarizing table of error functions for IA on CP811C - 300 over 3 different temperatures – Average Values**

|  | Freundlich | Single Langmuir | Double Langmuir | Sips | Toth | Redlich - Peterson |
|---|---|---|---|---|---|---|
| **Adjusted $R^2$** | 0.8634 | 0.9262 | 0.9221 | 0.9479 | 0.9236 | 0.9395 |
| **Chi-square $\chi^2$** | 129.51 | 80.06 | 77.42 | 209.30 | 77.50 | 67.94 |
| **HYBRYID** | 5055.99 | 2867.18 | 3177.56 | 239.23 | 2399.57 | 1767.70 |
| **MPSD** | 571.17 | 411.49 | 431.57 | 152.70 | 386.29 | 336.52 |
| **ARE** | 395.19 | 279.27 | 309.64 | 36.35 | 259.59 | 217.51 |

**Table A. 5: Summarizing table of error functions for FA on CBV 28014 over 3 different temperatures – Average Values**

|  | Freundlich | Single Langmuir | Double Langmuir | Sips | Toth | Redlich - Peterson |
|---|---|---|---|---|---|---|
| **Adjusted $R^2$** | 0.8439 | 0.8841 | 0.8751 | 0.8821 | 0.8775 | 0.8792 |
| **Chi-square $\chi^2$** | 117.73 | 97.41 | 94.97 | 89.87 | 97.50 | 96.00 |
| **HYBRYID** | 14426.01 | 7675.29 | 9983.23 | 4175.91 | 8514.86 | 8723.53 |
| **MPSD** | 979.69 | 719.34 | 818.77 | 574.26 | 752.40 | 770.20 |
| **ARE** | 538.13 | 392.26 | 472.80 | 286.89 | 425.01 | 429.22 |

**Table A. 6: Summarizing table of error functions for FA on CP811C-300 over 3 different temperatures – Average Values**

|  | Freundlich | Single Langmuir | Double Langmuir | Sips | Toth | Redlich - Peterson |
|---|---|---|---|---|---|---|
| **Adjusted R2** | 0.9263 | 0.9519 | 0.9504 | 0.9586 | 0.6860 | 0.6806 |
| **Chi-square $\chi 2$** | 39.29 | 20.84 | 16.94 | 15.56 | 34.58 | 31.96 |
| **HYBRYID** | 1092.06 | 421.90 | 348.64 | 121.07 | 1134.63 | 1164.25 |
| **MPSD** | 262.93 | 175.95 | 166.02 | 108.89 | 301.38 | 305.51 |
| **ARE** | 112.62 | 72.89 | 71.35 | 40.74 | 133.01 | 133.78 |

**Table A. 7: Summarizing table of error functions for MA on CBV 28014 over 3 different temperatures – Average Values**

|  | Freundlich | Single Langmuir | Double Langmuir | Sips | Toth | Redlich - Peterson |
|---|---|---|---|---|---|---|
| **Adjusted R2** | 0.7127 | 0.7340 | 0.6902 | 0.9075 | 0.7142 | 0.7399 |
| **Chi-square $\chi 2$** | 45.97 | 43.99 | 44.00 | 12.14 | 43.96 | 39.32 |
| **HYBRYID** | 389.06 | 387.98 | 447.88 | 74.87 | 413.79 | 386.46 |
| **MPSD** | 192.59 | 190.72 | 205.44 | 86.51 | 197.29 | 186.61 |
| **ARE** | 16.47 | 16.07 | 18.87 | 7.83 | 17.33 | 16.65 |

**Table A. 8: Summarizing table of error functions for MA on CP811C-300 over 3 different temperatures – Average Values**

|  | Freundlich | Single Langmuir | Double Langmuir | Sips | Toth | Redlich - Peterson |
|---|---|---|---|---|---|---|
| **Adjusted $R^2$** | 0.6750 | 0.6886 | 0.6557 | 0.8297 | 0.6719 | 0.7132 |
| **Chi-square $\chi^2$** | 67.15 | 65.05 | 64.89 | 26.30 | 65.05 | 57.01 |
| **HYBRYID** | 569.62 | 602.12 | 673.55 | 160.04 | 634.76 | 664.77 |
| **MPSD** | 209.72 | 212.85 | 224.16 | 112.37 | 218.46 | 218.34 |
| **ARE** | 35.74 | 36.78 | 40.98 | 16.38 | 38.79 | 40.09 |

**Table A. 9: Summarizing table of error functions for CA on CBV 28014 over 2 different temperatures – Average Values**

|  | Freundlich | Single Langmuir | Double Langmuir | Sips | Toth | Redlich - Peterson |
|---|---|---|---|---|---|---|
| **Adjusted R2** | 0.7512 | 0.7513 | 0.7180 | 0.7360 | 0.7351 | 0.7419 |
| **Chi-square $\chi 2$** | 72.15 | 72.55 | 69.61 | 77.02 | 72.55 | 69.92 |
| **HYBRYID** | 933.16 | 884.59 | 1070.09 | 922.29 | 942.34 | 1046.67 |
| **MPSD** | 301.14 | 291.28 | 320.91 | 299.82 | 300.58 | 316.35 |
| **ARE** | 114.87 | 111.12 | 132.09 | 115.95 | 118.38 | 125.72 |

**Table A. 10: Summarizing table of error functions for CA on CP811C-300 over 2 different temperatures – Average Values**

|  | Freundlich | Single Langmuir | Double Langmuir | Sips | Toth | Redlich - Peterson |
|---|---|---|---|---|---|---|
| **Adjusted R2** | 0.8656 | 0.8673 | 0.8429 | 0.8623 | 0.8586 | 0.8637 |
| **Chi-square $\chi 2$** | 44.70 | 45.24 | 44.69 | 44.65 | 45.24 | 44.11 |
| **HYBRYID** | 434.20 | 401.57 | 503.67 | 440.03 | 425.96 | 437.88 |
| **MPSD** | 203.92 | 197.05 | 221.38 | 204.50 | 203.21 | 203.91 |
| **ARE** | 49.59 | 46.89 | 56.61 | 52.06 | 49.83 | 51.63 |

## 8.1.  Adsorption Isotherms
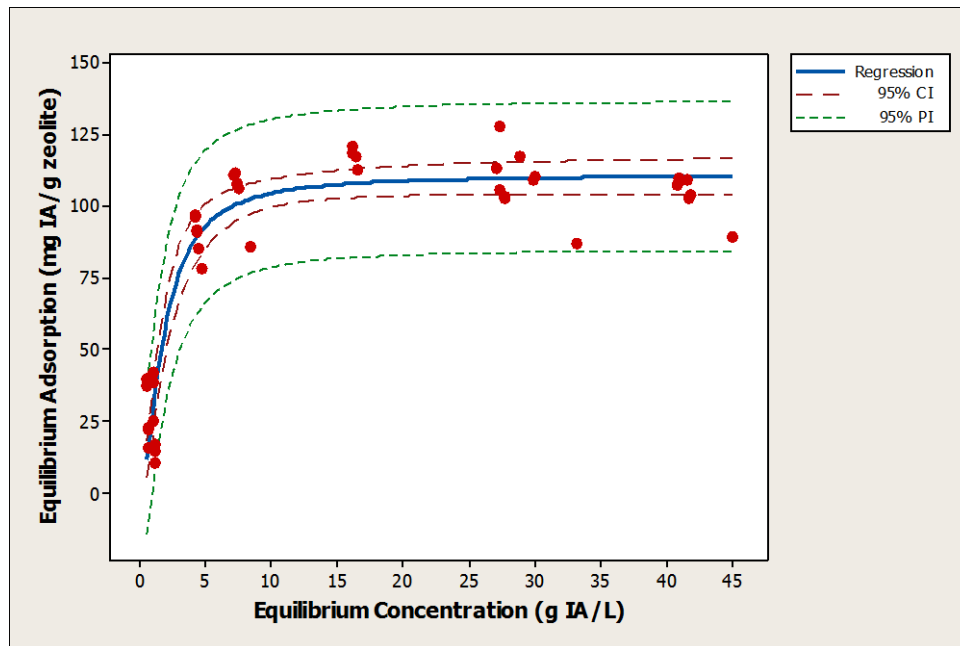


Figure A. 1: Adsorption of IA on CBV-28014 at 25ºC, Note: only volumetric concentration was measured
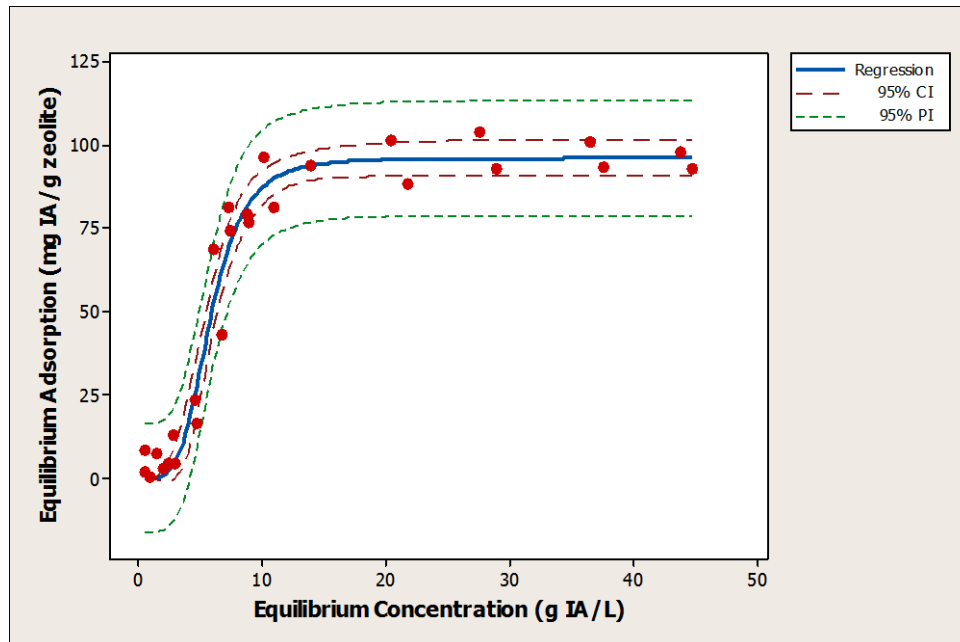


Figure A. 2: Adsorption of IA on CBV-28014 at 50ºC, Note: only volumetric concentration was measured
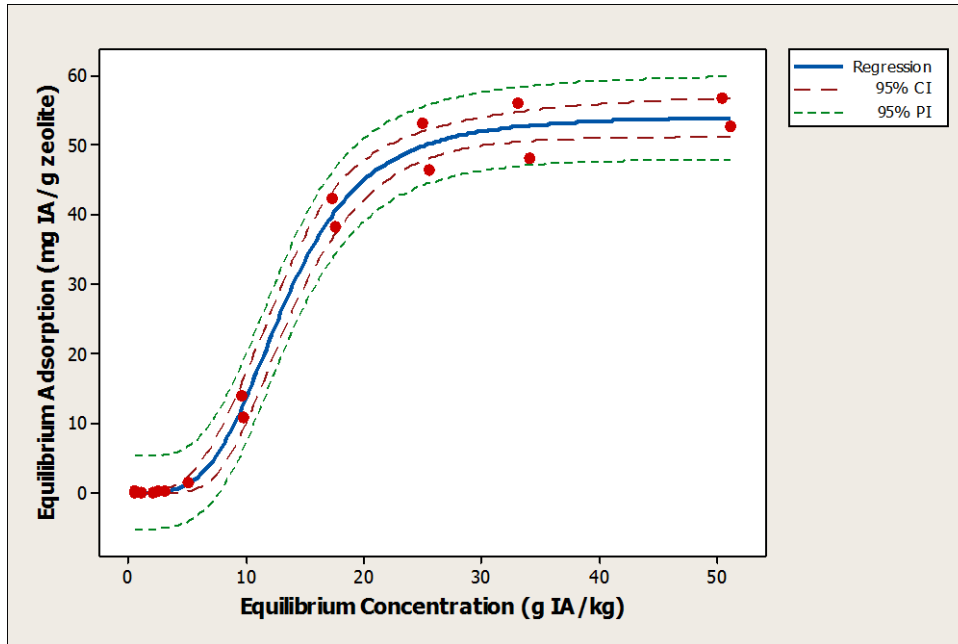
**Figure A. 3: Adsorption of IA on CBV-28014 at 70ºC**

**Table A. 11: Sips parameter estimation for IA on CBV-28014 at 25ºC, 50ºC and 70ºC**

| Parameter | Estimate | | | Standard Error | | | 95% Confidence Interval | | | | | |
| | 25 | 50 | 70 | 25 | 50 | 70 | 25 | | 50 | | 70 | |
| | | | | | | | Lower | Upper | Lower | Upper | Lower | Upper |
| Ks | 42.56 | $5.555 \cdot 10^{-2}$ | $2.720 \cdot 10^{-3}$ | 8.08 | $6.49 \cdot 10^{-2}$ | $2.963 \cdot 10^{-3}$ | 25.58 | 62.32 | 0.00191 | 0.4749 | - | - |
| Bs | 1.626 | 4.228 | 3.834 | 0.23 | 0.6422 | 0.4268 | 1.225 | 2.189 | 3.047 | - | - | - |
| As | 0.383 | $5.772 \cdot 10^{-4}$ | $5.010 \cdot 10^{-5}$ | 0.07 | $7 \cdot 10^{-4}$ | $5.39 \cdot 10^{-5}$ | 0.231 | 0.566 | - | - | - | - |
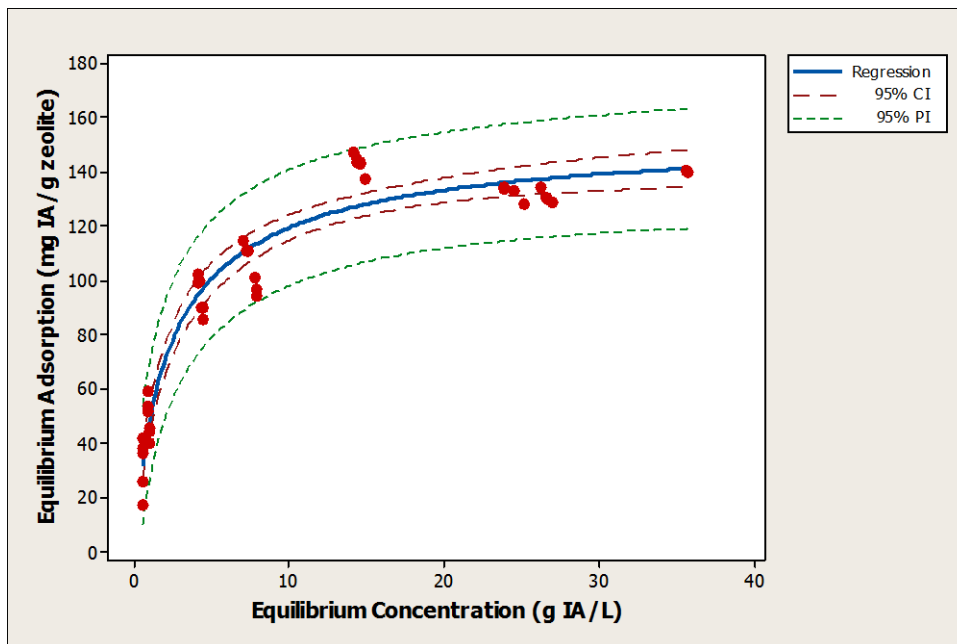


**Figure A. 4: Adsorption of IA on CP811C-300 at 25ºC, Note: only volumetric concentration was measured**
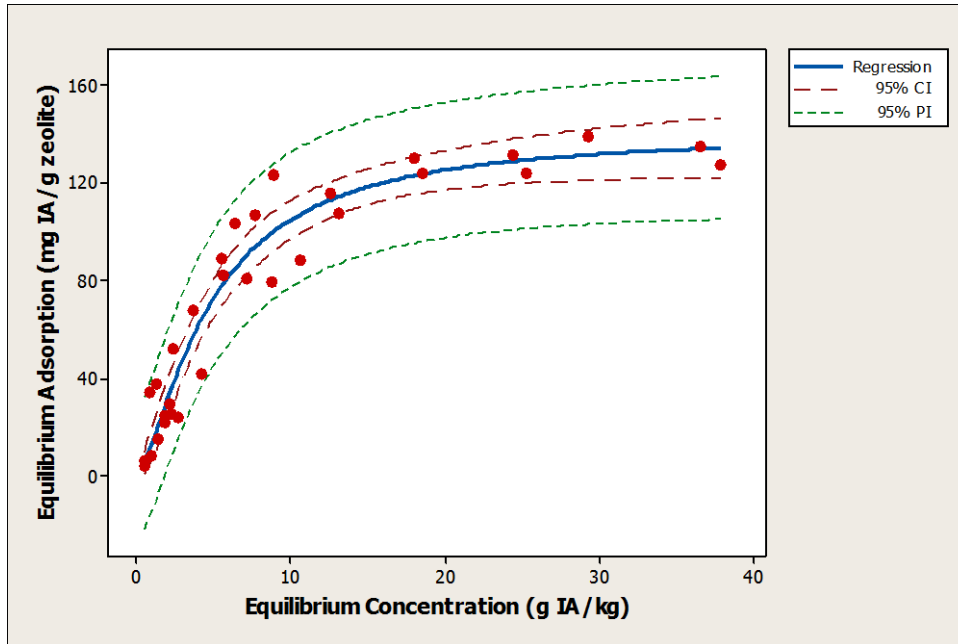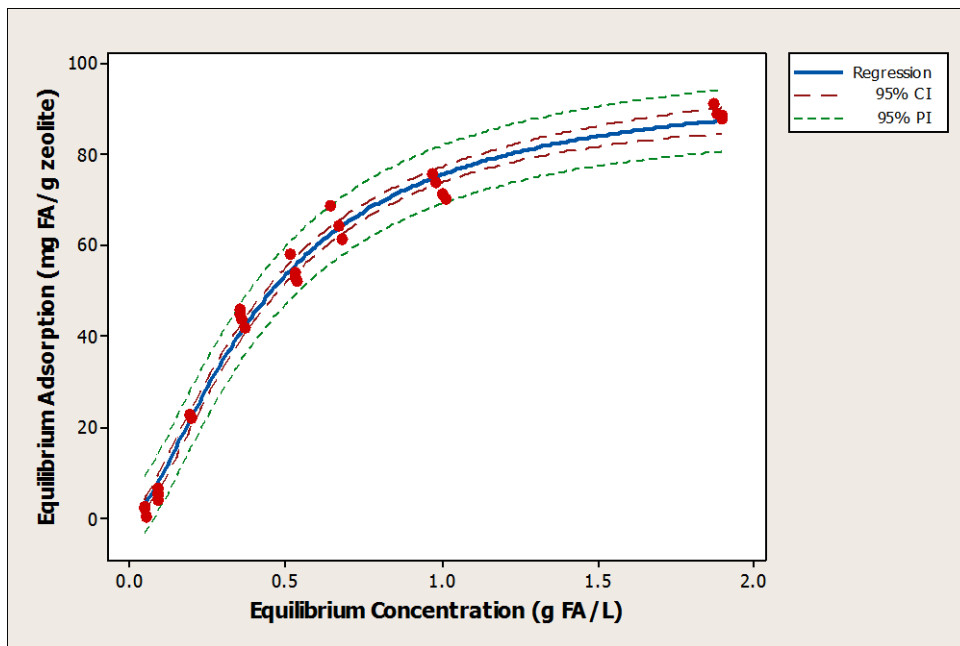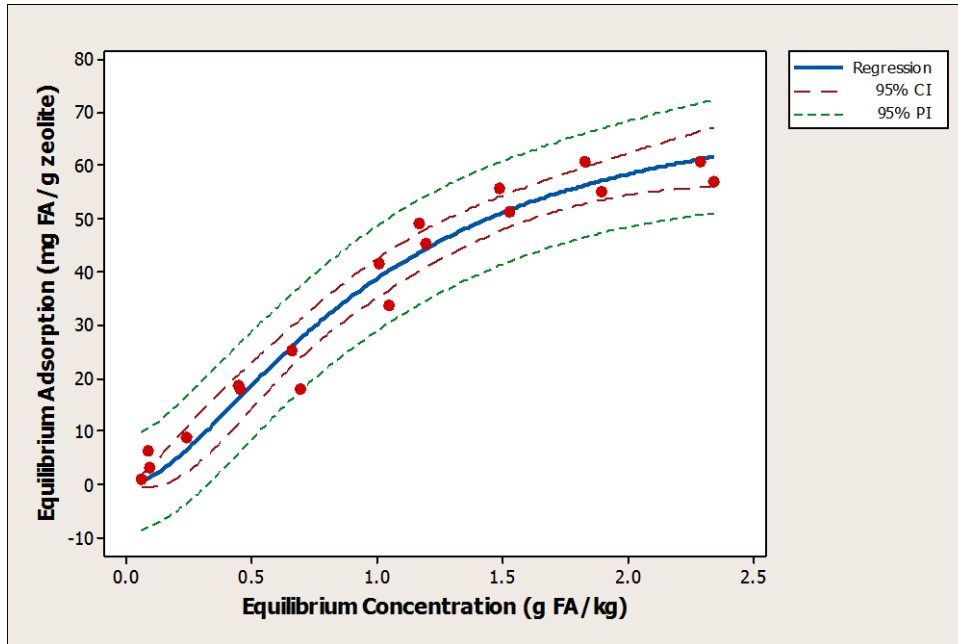
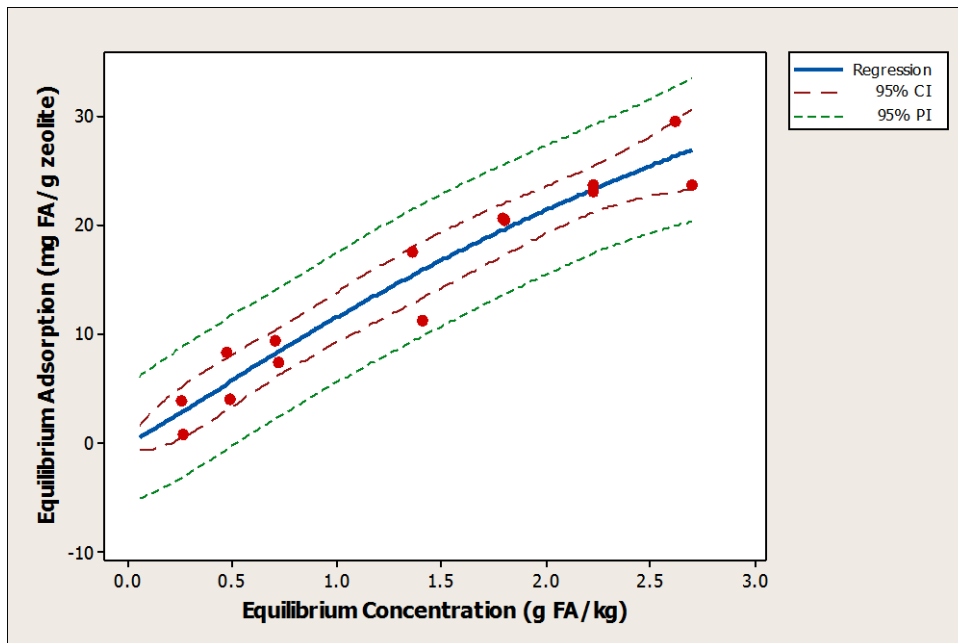**Figure A. 5: Adsorption of IA on CP811C-300 at 50ºC**
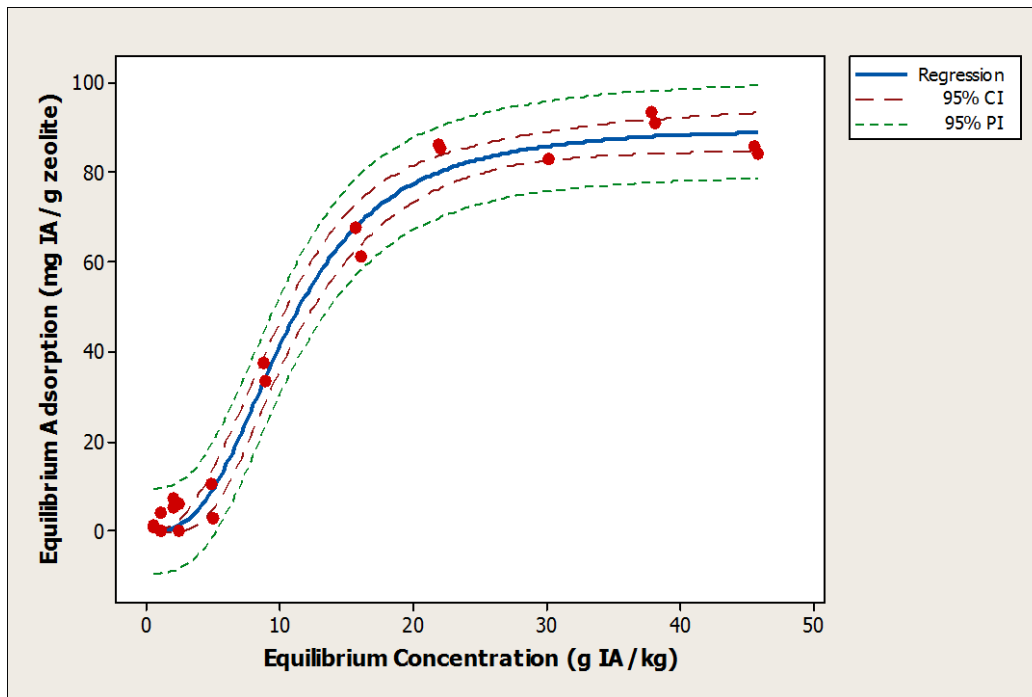


**Figure A. 6: Adsorption of IA on CP811C-300 at 70ºC**

**Table A. 12: Sips parameter estimation for IA on CP811C-300 at 25ºC, 50ºC and 70ºC**

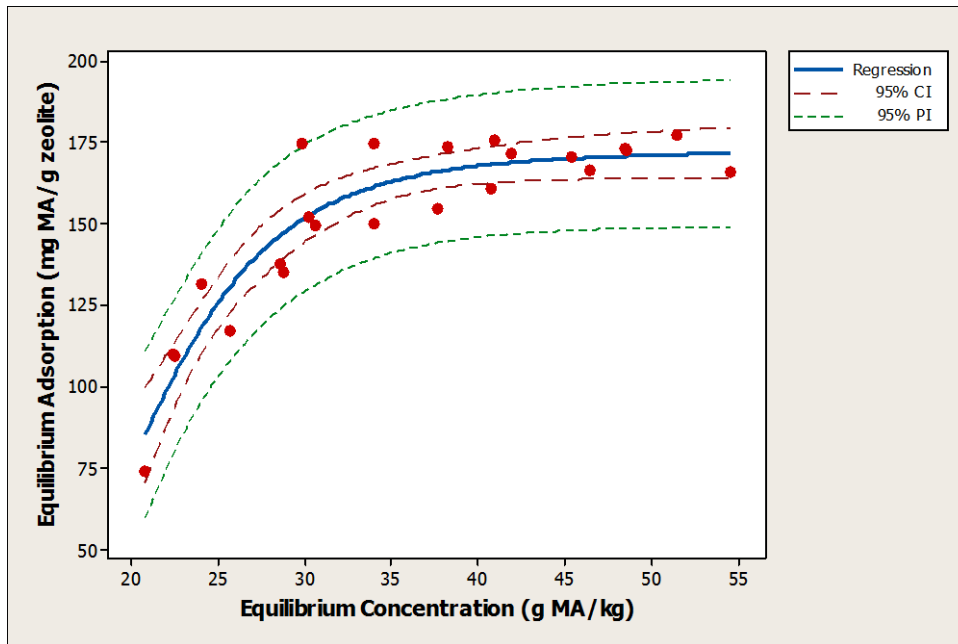| Parameter | Estimate | | | Standard Error | | | 95% Confidence Interval | | | | | |
|---|---|---|---|---|---|---|---|---|---|---|---|---|
| | | | | | | | 25 | | 50 | | 70 | |
| | 25 | 50 | 70 | 25 | 50 | 70 | Lower | Upper | Lower | Upper | Lower | Upper |
| Ks | 73.21 | 14.83 | 0.1156 | 6.40 | 4.17 | 0.0882 | 60.94 | 87.41 | 7.11 | 25.03 | - | 0.4763 |
| βs | 0.8453 | 1.440 | 2.821 | 0.1014 | 0.214 | 0.332 | 0.6568 | 1.051 | 1.028 | 1.984 | 2.206 | - |
| αs | 0.4695 | 0.1051 | 0.00128 | 0.0536 | 0.0266 | 0.00095 | 0.3733 | 0.5905 | 0.05364 | 0.1677 | - | 0.005045 |
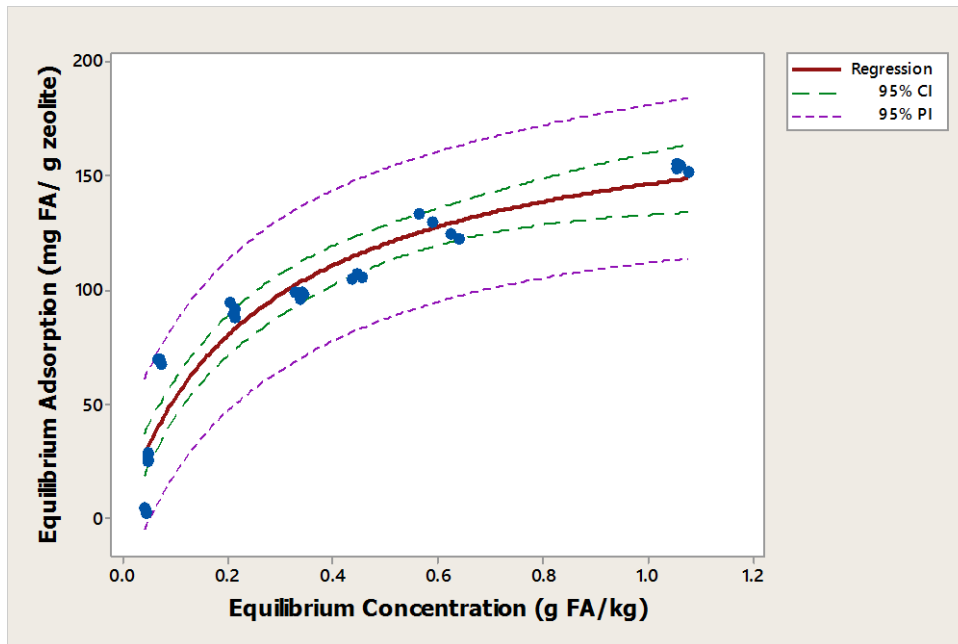
**Figure A. 7: Adsorption of FA on CBV-28014 at 25ºC**
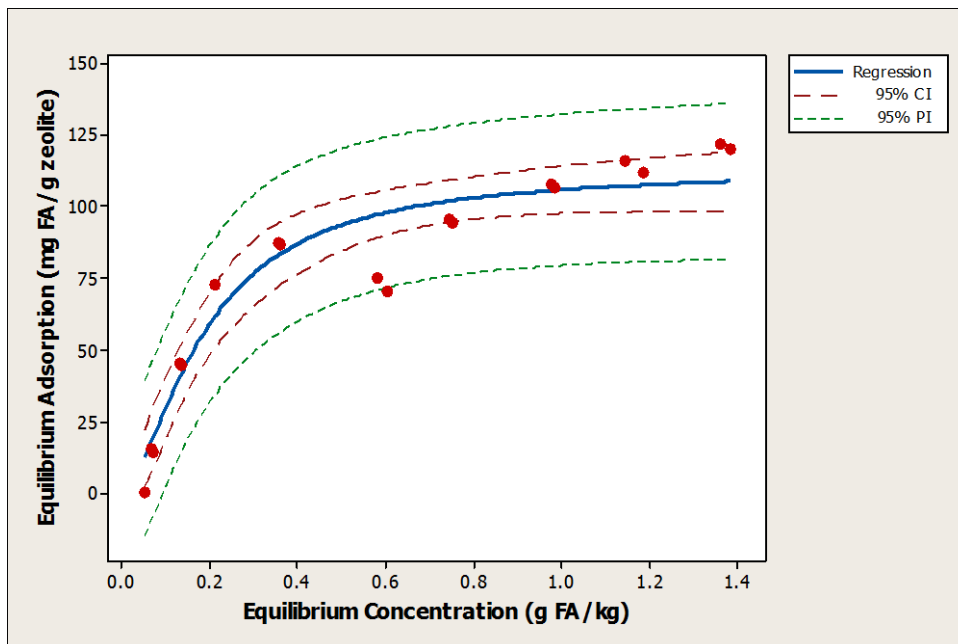


**Figure A. 8: Adsorption of FA on CBV-28014 at 50ºC**
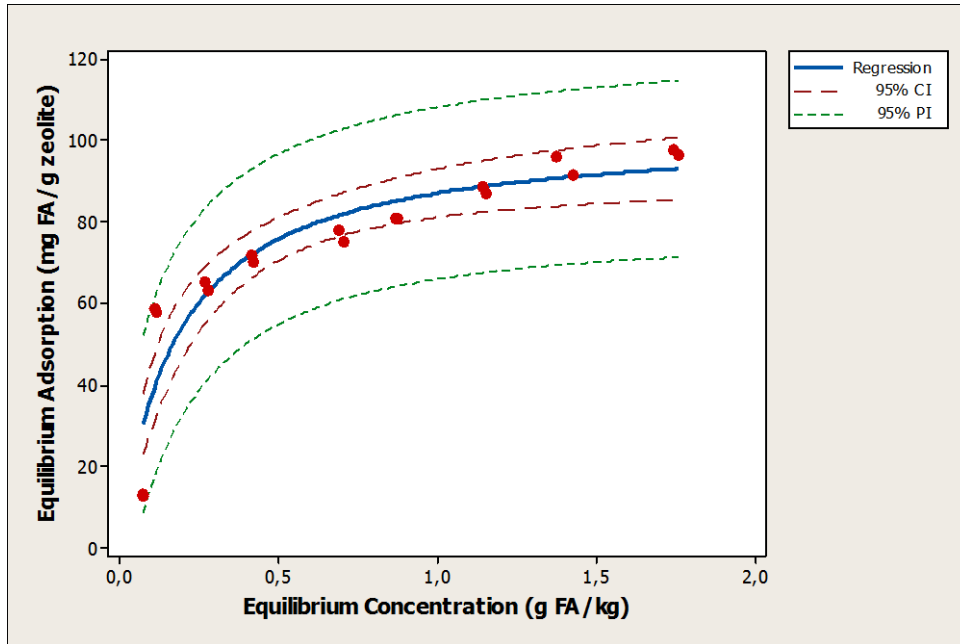
**Figure A. 9: Adsorption of FA on CBV-28014 at 70ºC**

**Table A. 13: Sips parameter estimation for FA on CBV-28014 at 25ºC, 50ºC and 70ºC**

| Parameter | Estimate | | | Standard Error | | | 95% Confidence Interval | | | | | |
|---|---|---|---|---|---|---|---|---|---|---|---|---|
| | 25 | 50 | 70 | 25 | 50 | 70 | 25 | | 50 | | 70 | |
| | | | | | | | Lower | Upper | Lower | Upper | Lower | Upper |
| Ks | 598.7 | 1654 | 695.2 | 280.4 | 1208 | 528.4 | 219.2 | 2010 | - | 40142 | 99.59 | - |
| βs | 0.921 | 1.607 | 1.071 | 0.181 | 0.36 | 0.336 | 0.564 | 1.36 | 0.8196 | 3.1 | 0.3416 | - |
| αs | 3.088 | 14.60 | 6.969 | 2.024 | 11.57 | 6.063 | 0.420 | 13.87 | - | 397.6 | 0.1680 | - |



**Figure A. 10: Adsorption of FA on CP811C-300 at 25ºC, Note: only volumetric concentration was measured**

**Figure A. 11: Adsorption of FA on CP811C-300 at 50ºC**



**Figure A. 12: Adsorption of FA on CP811C-300 at 70ºC**

**Table 15: Sips parameter estimation for FA on CP811C-300 at 25ºC, 50ºC and 70ºC**

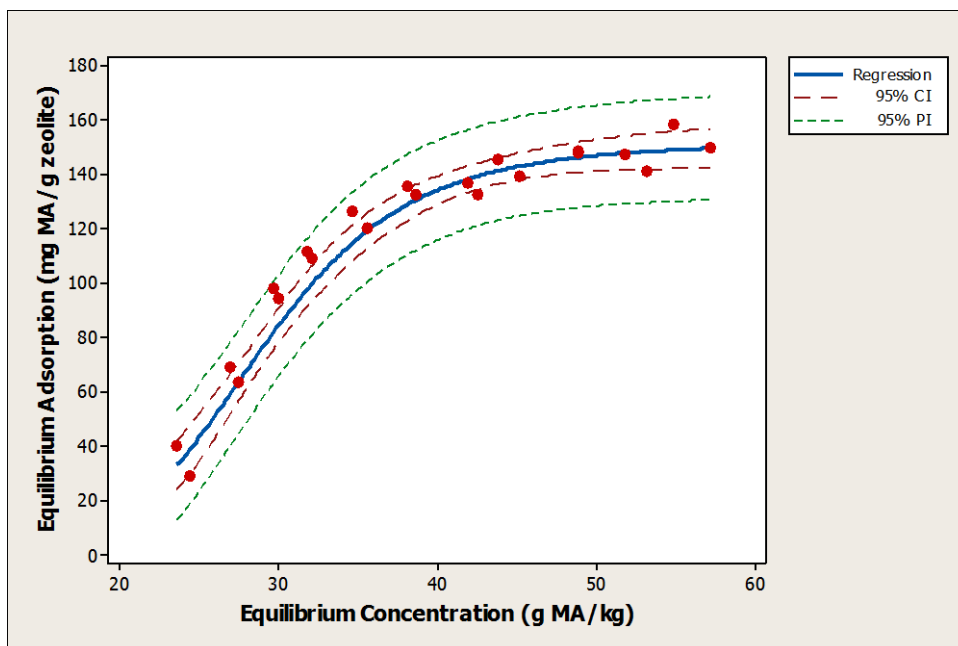| Parameter | Estimate | | | Standard Error | | | 95% Confidence Interval | | | | | |
|---|---|---|---|---|---|---|---|---|---|---|---|---|
| | | | | | | | 25 | | 50 | | 70 | |
| | 25 | 50 | 70 | 25 | 50 | 70 | Lower | Upper | Lower | Upper | Lower | Upper |
| Ks | 348.6 | 80.13 | 13.64 | 40.03 | 17.88 | 4.093 | 276.7 | 446.9 | 49.67 | 129.8 | 4.896 | 25.89 |
| βs | 1.532 | 1.682 | 1.131 | 0.0871 | 0.3409 | 0.4133 | 1.366 | 1.717 | 1.004 | 2.596 | - | 2.144 |
| αs | 3.606 | 1.058 | 0.1818 | 0.5158 | 0.3869 | 0.2914 | 2.681 | 4.882 | 0.3534 | 2.099 | - | 0.8991 |

**Figure A. 13: Adsorption of MA on CBV-28014 at 25ºC**


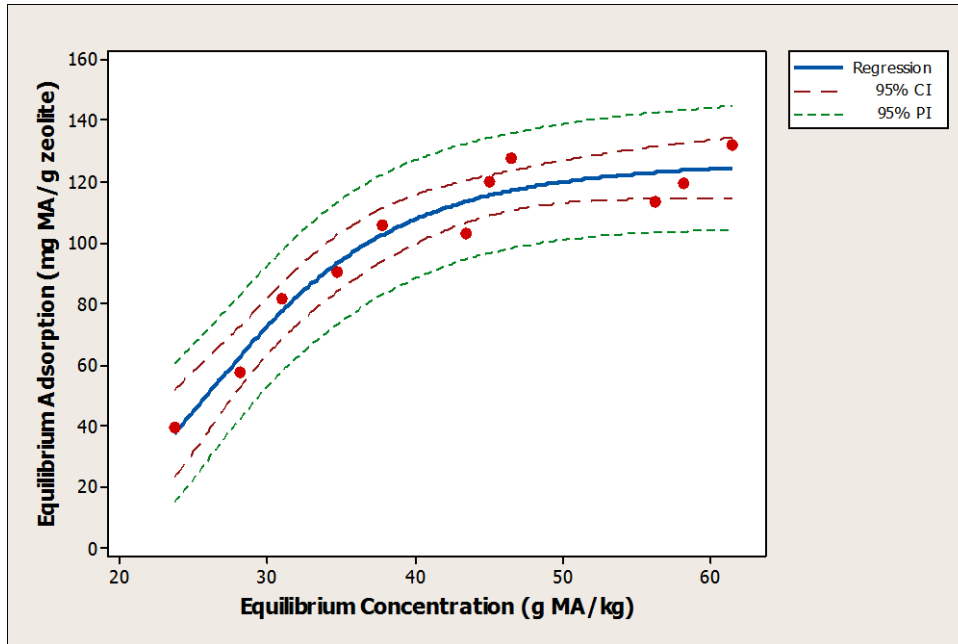
**Figure A. 14: Adsorption of MA on CBV-28014 at 50ºC**

**Figure A. 15: Adsorption of MA on CBV-28014 at 70ºC**

**Table 16: Sips parameter estimation for MA on CBV-28014 at 25ºC, 50ºC and 70ºC**

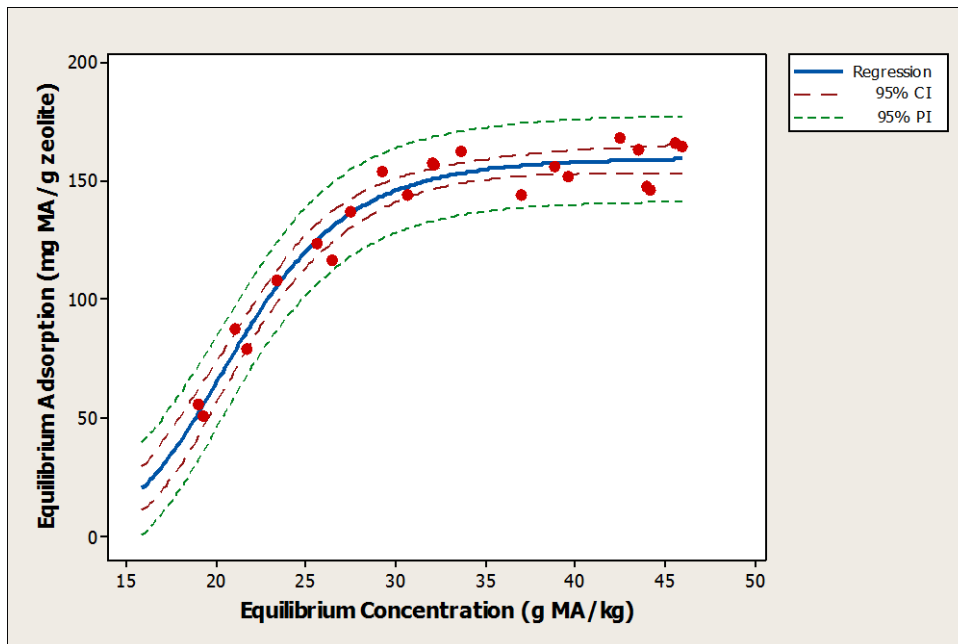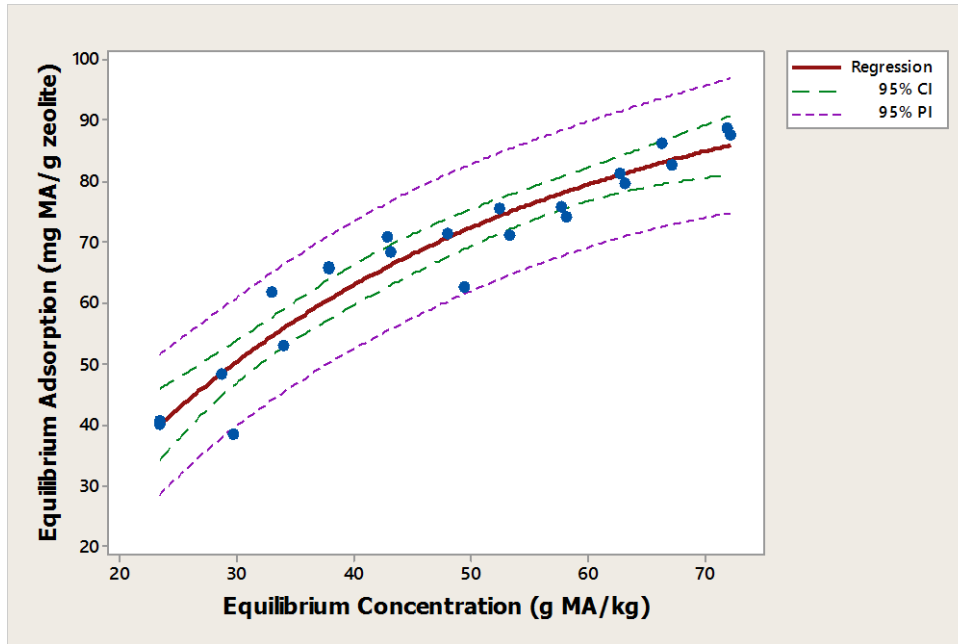| Parameter | Estimate | | | Standard Error | | |
|---|---|---|---|---|---|---|
| | 25 | 50 | 70 | 25 | 50 | 70 |
| **Ks** | $9.565 \cdot 10^{-6}$ | $9.853 \cdot 10^{-8}$ | $9.422 \cdot 10^{-6}$ | - | - | - |
| **βs** | 5.5 | 6.287 | 4.914 | 1.053 | 0.7490 | 0.9955 |
| **αs** | $5.531 \cdot 10^{-8}$ | $6.496 \cdot 10^{-10}$ | $7.413 \cdot 10^{-8}$ | - | - | - |



**Figure A. 16: Adsorption of MA on CP811C-300 at 25ºC**
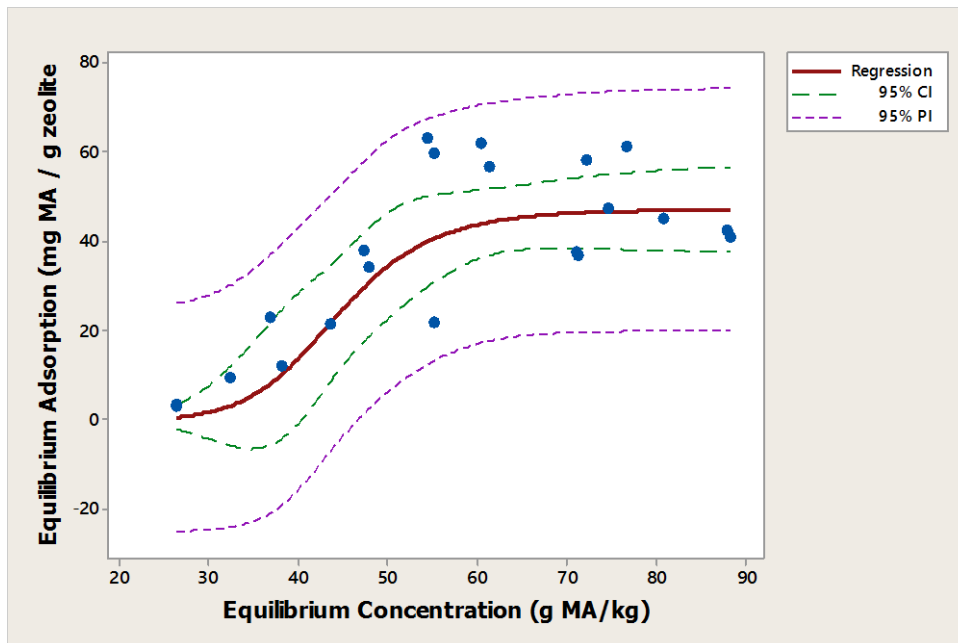
**Figure A. 17: Adsorption of MA on CP811C-300 at 50ºC**



**Figure A. 18: Adsorption of MA on CP811C-300 at 70ºC**

**Table A. 14: Sips parameter estimation for MA adsorption on CP811C-300 at 25ºC, 50ºC and 70ºC**

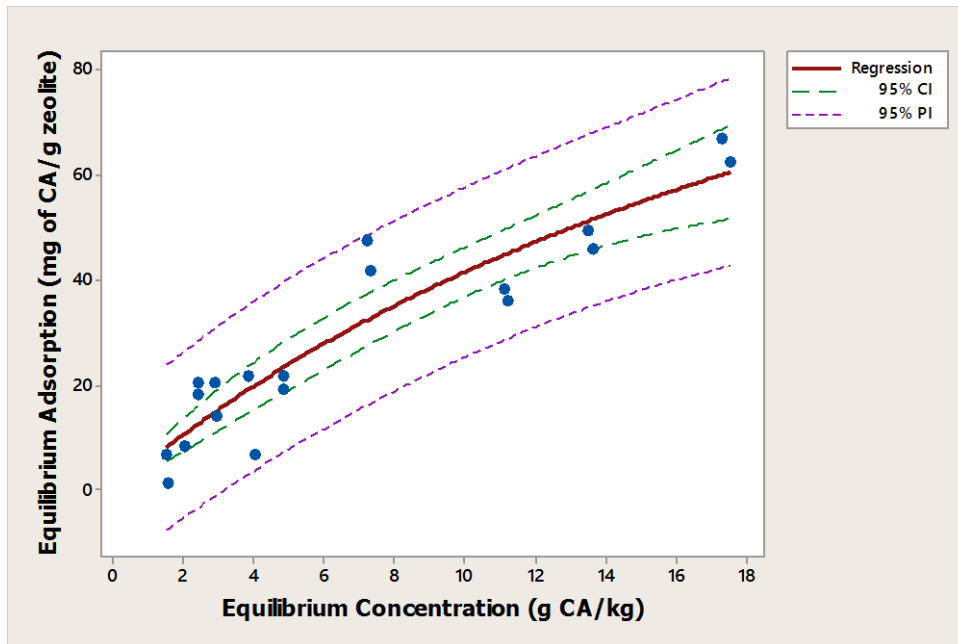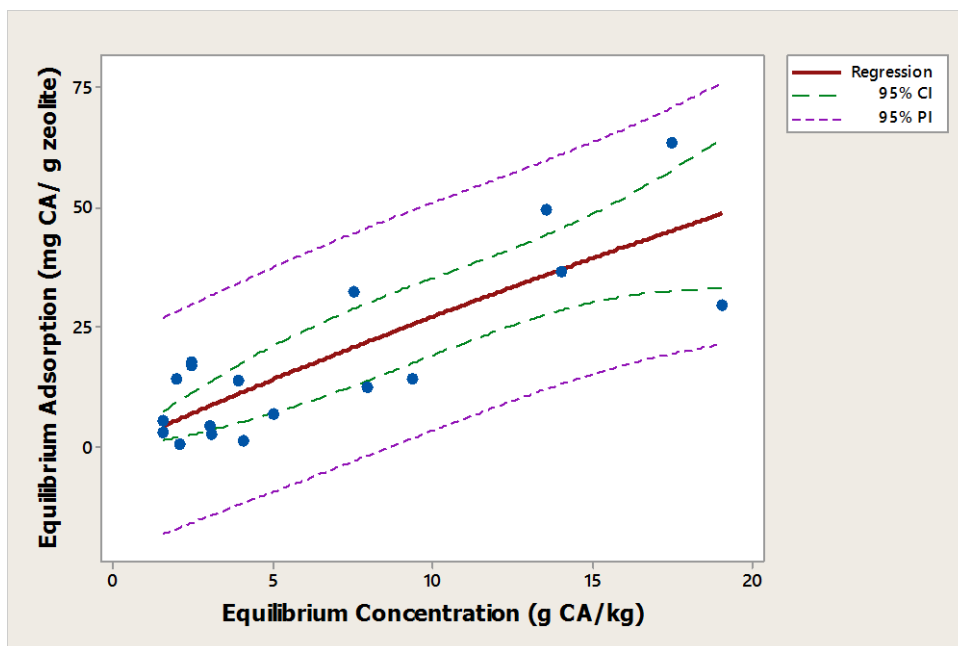| Parameter | Estimate | | | Standard Error | | |
|:---:|:---:|:---:|:---:|:---:|:---:|:---:|
| | 25 | 50 | 70 | 25 | 50 | 70 |
| **Ks** | $2.256 \cdot 10^{-7}$ | 0.4680 | $5.7 \cdot 10^{-7}$ | - | 0.7320 | - |
| **βs** | 6.679 | 1.5468 | 4.93 | 0.7539 | 0.5058 | - |
| **αs** | $1.407 \cdot 10^{-9}$ | 0.0041 | $1.085 \cdot 10^{-8}$ | - | 0.0056 | - |

**Figure A. 19: Adsorption of CA on CBV-28014 at 25ºC**



**Figure A. 20: Adsorption of CA on CBV-28014 at 50ºC**

**Table A. 15: Sips parameter estimation for CA on CBV-28014 at 25ºC and 50ºC**

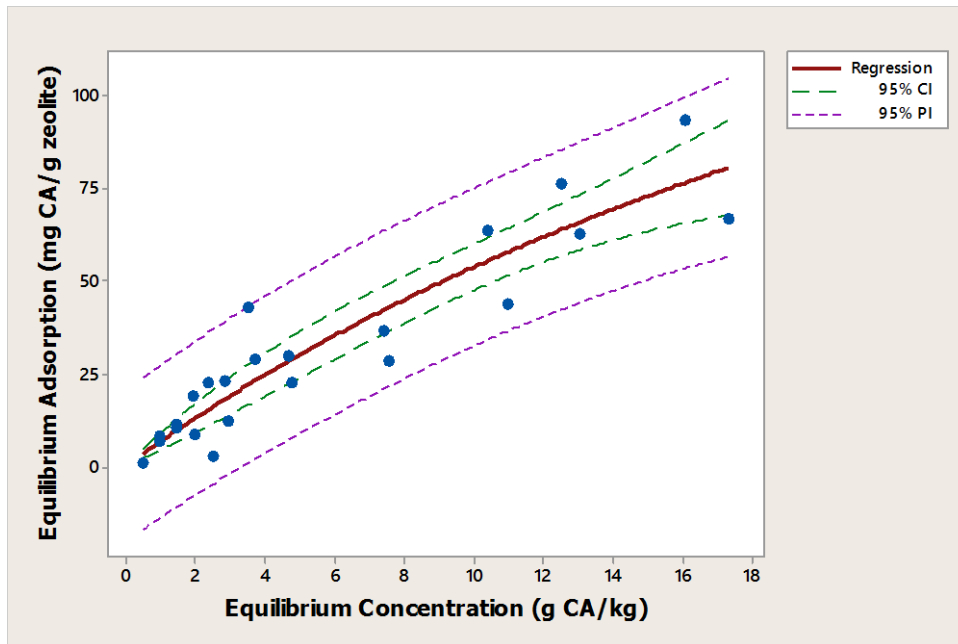|  | Estimate | | Standard Error | |
|---|---|---|---|---|
| **Parameter** | 25 | 50 | 25 | 50 |
| **qsat** | 153.6 | 373.3 | 59.06 | 1134 |
| **$k_L$** | 0.03708 | 0.007886 | 0.02038 | 0.02659 |

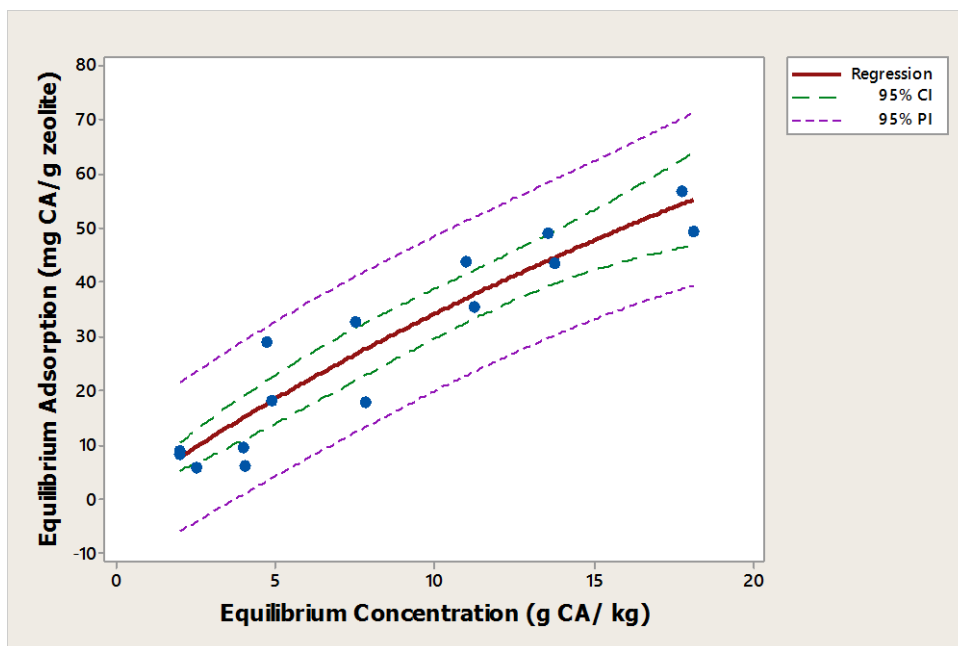**Figure A. 21: Adsorption of CA on CP811C-300 at 25ºC**



**Figure A. 22: Adsorption of CA on CP811C-300 at 50ºC**

**Table A. 16: Single Langmuir parameter estimation for CA adsorption on CP811C-300 at 25ºC and 50ºC**

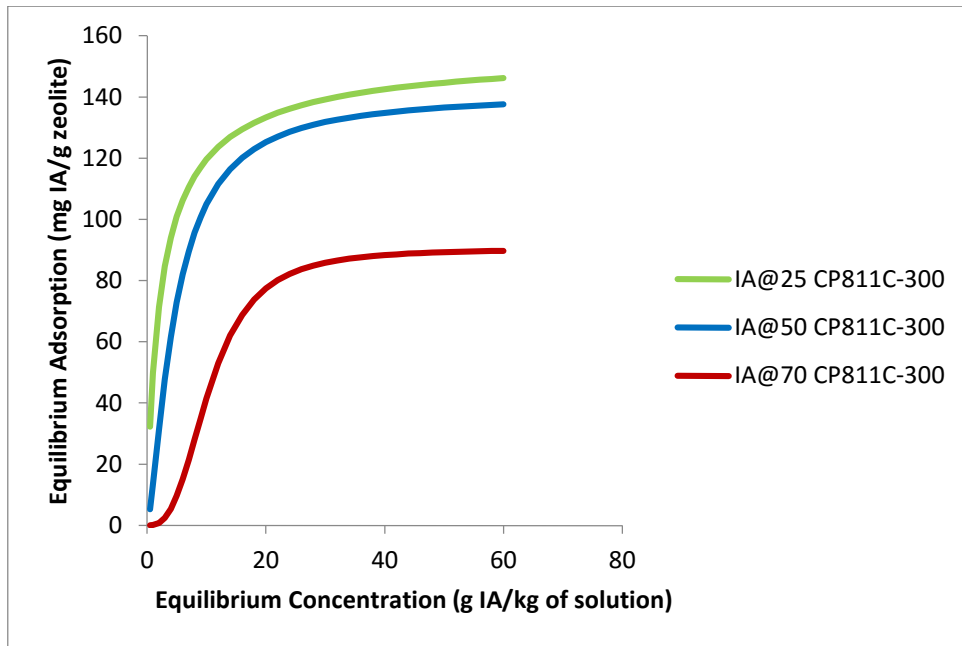|  | **Estimate** | | **Standard Error** | |
| --- | --- | --- | --- | --- |
| **Parameter** | 25 | 50 | 25 | 50 |
| **qsat** | 252.5 | 230.0 | 135.6 | 177.2 |
| **$k_L$** | 0.02700 | 0.01748 | 0.01896 | 0.01654 |

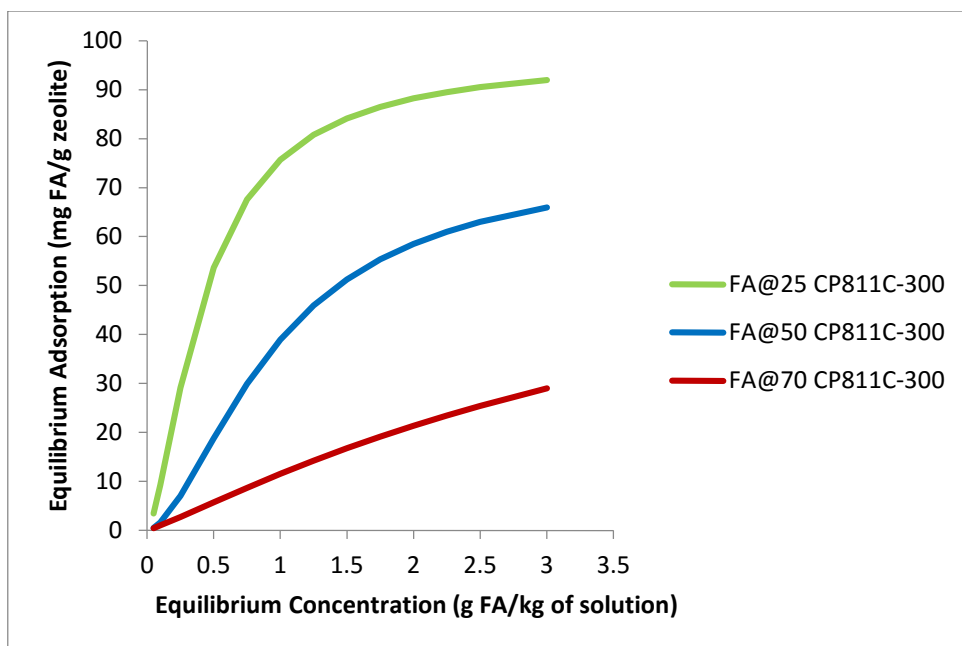**Figure A. 23: IA Adsorption on CP811C-300 at 3 different temperatures**



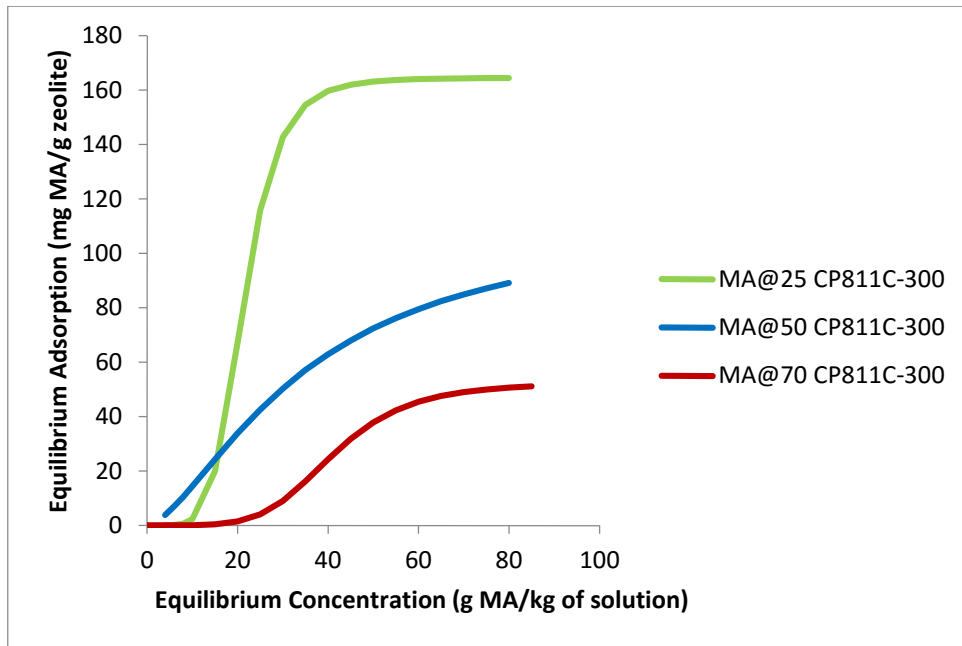**Figure A. 24: FA adsorption on CP811C-300 at 3 different temperatures**

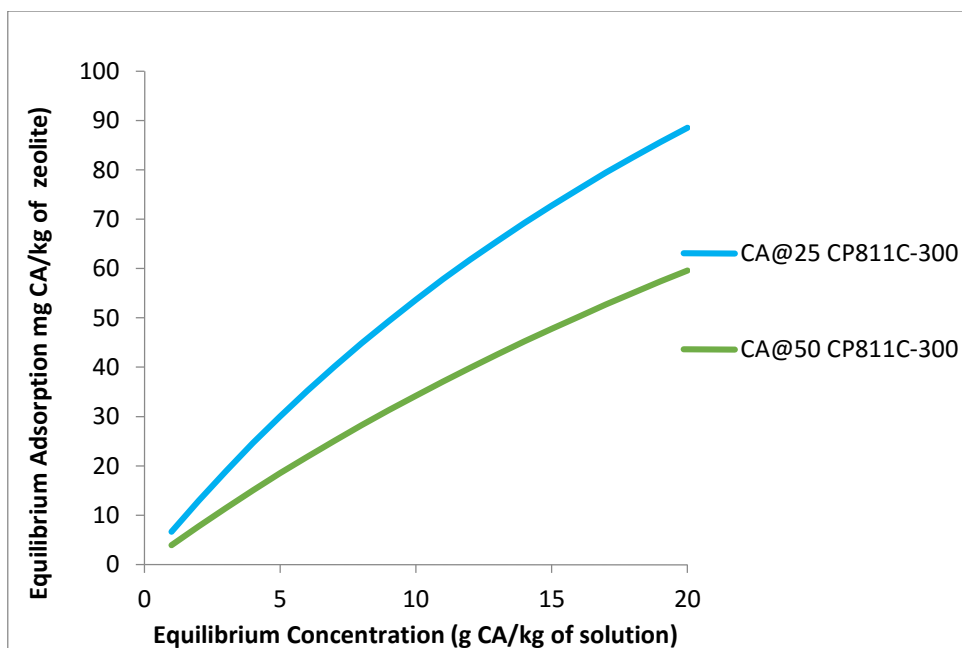**Figure A. 25: MA adsorption on CP811C-300 at 3 different temperatures**



**Figure A. 26: CA adsorption on CP811C-300 at 2 different temperatures**

**Table A. 17: Comparative table of the parameters for IA, FA, MA on CP811C – 300 at 3 different temperatures**

| Parameter | IA | | | FA | | | MA | | |
|---|---|---|---|---|---|---|---|---|---|
| | 25°C | 50°C | 70°C | 25°C | 50°C | 70°C | 25°C | 50°C | 70°C |
| Ks | 73.21 | 14.83 | 0.1156 | 348.6 | 80.13 | 13.64 | $2.256 \cdot 10^{-7}$ | 0.4680 | $5.7 \cdot 10^{-7}$ |
| βs | 0.8453 | 1.440 | 2.821 | 1.532 | 1.682 | 1.131 | 6.678 | 1.547 | 4.930 |
| αs | 0.4695 | 0.1051 | 0.00128 | 3.606 | 1.058 | 0.1818 | $1.407 \cdot 10^{-9}$ | 0.0041 | 1.085E-08 |

**Table A. 18: Parameters for CA on CP811C – 300 at 2 different temperatures**

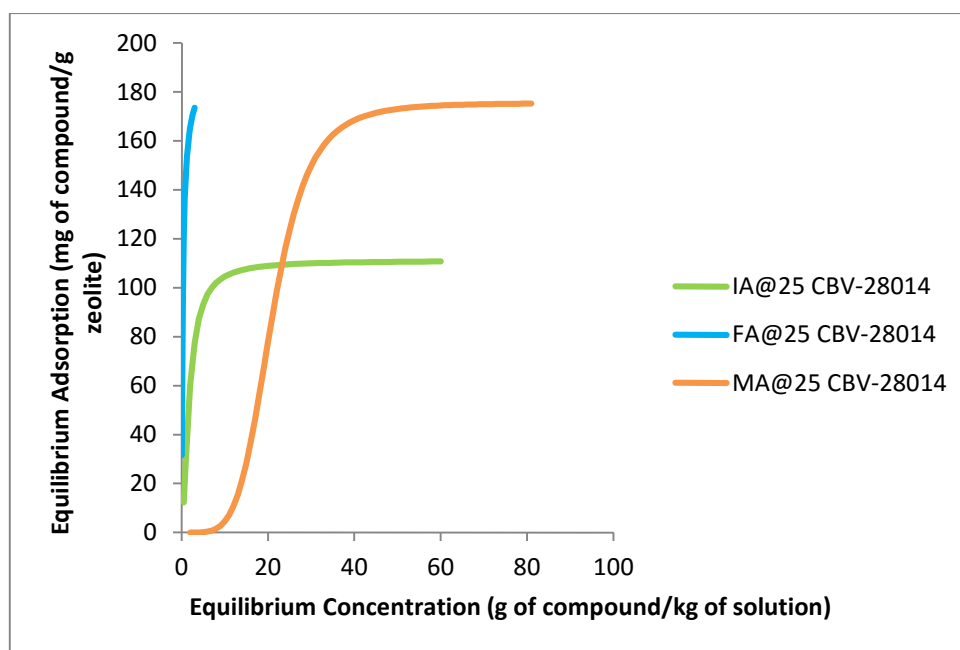| Parameter | Estimate | |
|---|---|---|
| | 25°C | 50°C |
| qsat | 252.5 | 230.0 |
| $k_L$ | 0.02700 | 0.01748 |



**Figure A. 27: Adsorption of compounds at 25°C on CBV-28014**
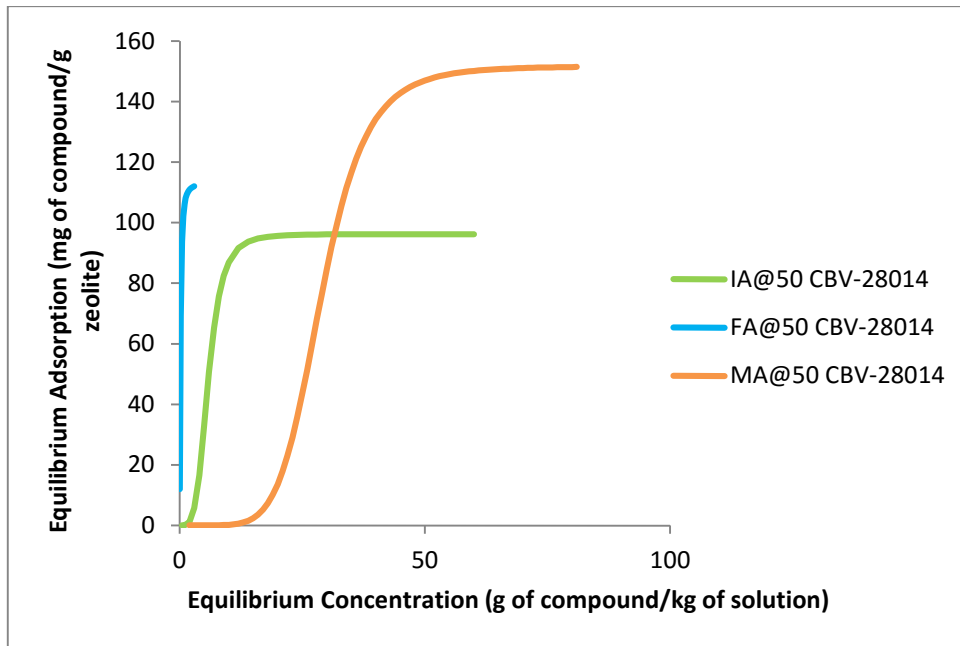
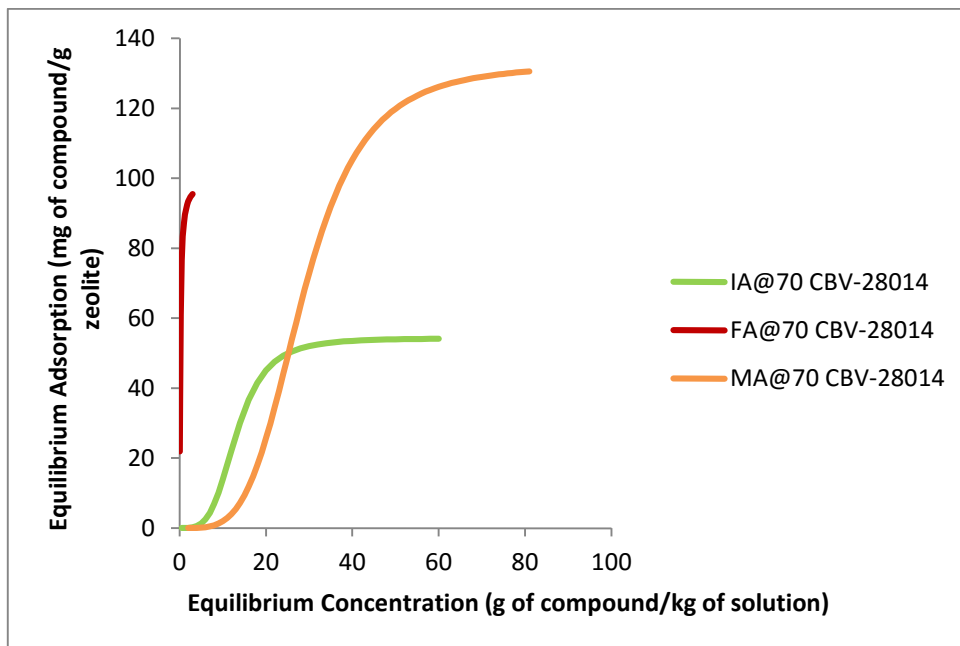**Figure A. 28: Adsorption of compounds at 50 °C on CBV-28014**


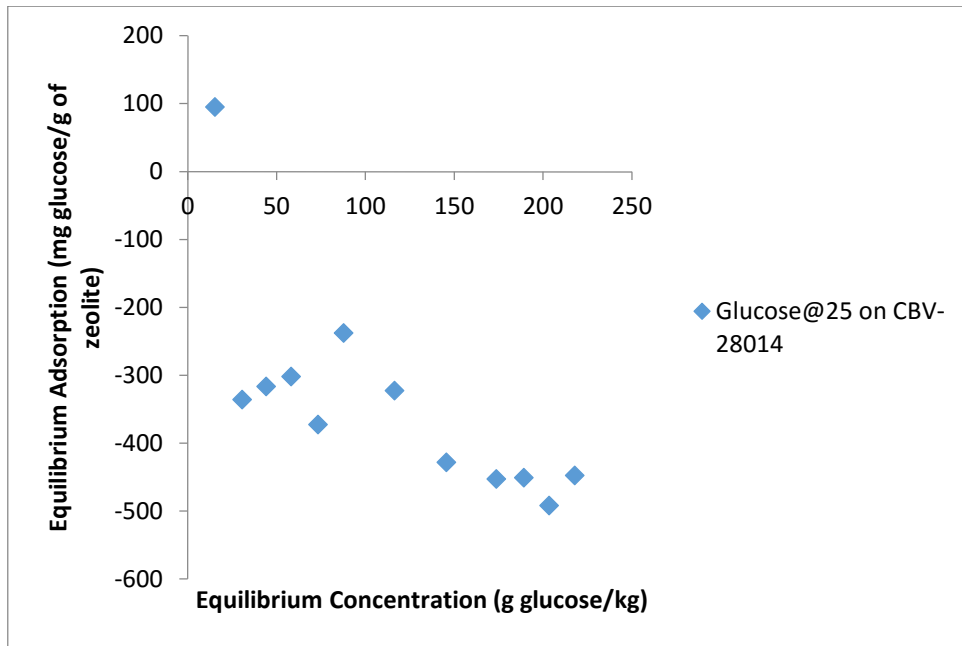
**Figure A. 29: Adsorption of compounds at 70 °C on CBV-28014**

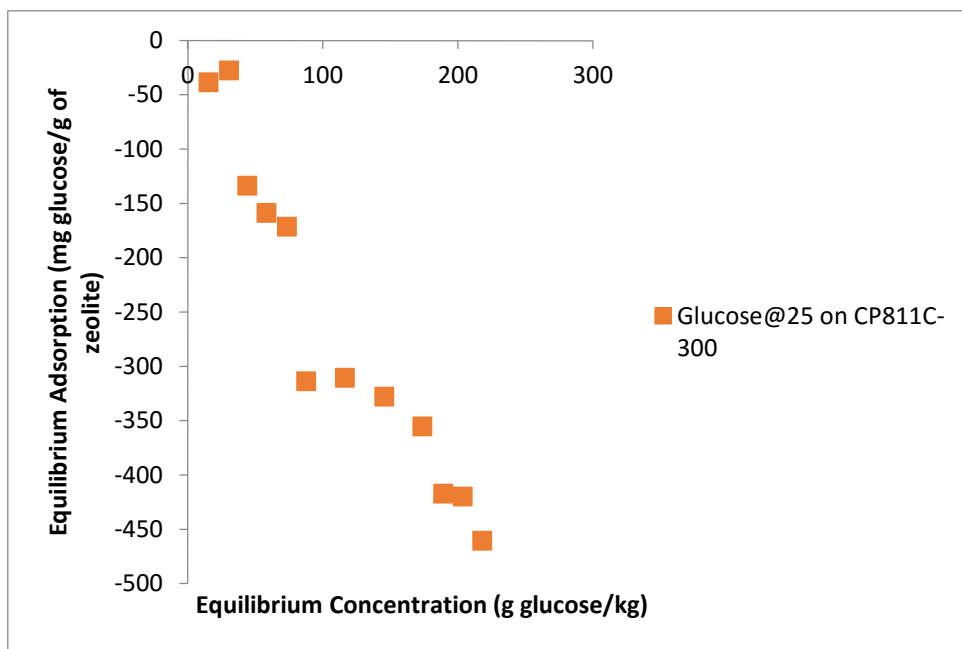**Figure A. 30: Glucose adsorption at 25 ºC on CBV-28014**



**Figure A. 31: Glucose adsorption at 25 ºC on CP811C-300**

## 9. Literature Cited [1-40, 42, 44-77]

1. Roa Engel, C.A., et al., *Fumaric acid production by fermentation.* Applied Microbiology and Biotechnology, 2008. **78**(3): p. 379-389.
2. Energy, U.S.D.o.E.E.E.a.R., *Top Value Added Chemicals from Biomass Results of Screening for Potential Candidates from Sugars and Synthesis Gas.* **I**.
3. *GESTIS Substance Database*.
4. Dang, L., et al., *Solubility of Fumaric Acid in Propan-2-ol, Ethanol, Acetone, Propan-1-ol, and Water.* Journal of Chemical & Engineering Data, 2009. **54**(11): p. 3112-3113.
5. Information, N.C.f.B., *PubChem Compound Database, Fumaric Acid*.
6. Grand View Research, M.R.C., *Global Fumaric Acid Market By Application (Food & Beverages, Rosin Paper Sizes, UPR, Alkyd Resins) Expected To Reach USD 764.8 Million By 2020.* March 2015.
7. *Determination of market potential for selected platform chemicals Itaconic acid, Succinic acid, 2,5-Furandicarboxylic acid.* Bioconversion and Separation, 2013.
8. Research, T.M., *Itaconic Acid Market is Expected to Reach US$ 204.6 Mn by 2023.* 2015.
9. Zhang, K., B. Zhang, and S.-T. Yang, *Production of Citric, Itaconic, Fumaric, and Malic Acids in Filamentous Fungal Fermentations*, in *Bioprocessing Technologies in Biorefinery for Sustainable Production of Fuels, Chemicals, and Polymers*. 2013, John Wiley & Sons, Inc. p. 375-398.
10. Okabe, M., et al., *Biotechnological production of itaconic acid and its biosynthesis in Aspergillus terreus.* Applied Microbiology and Biotechnology, 2009. **84**(4): p. 597-606.
11. Zhang, X.-X., F. Ma, and D.-J. Lee, *Recovery of itaconic acid from supersaturated waste fermentation liquor.* Journal of the Taiwan Institute of Chemical Engineers, 2009. **40**(5): p. 583-585.
12. Cao, N., et al., *Simultaneous Production and Recovery of Fumaric Acid from Immobilized Rhizopus oryzae with a Rotary Biofilm Contactor and an Adsorption Column.* Appl Environ Microbiol, 1996. **62**(8): p. 2926-31.
13. Zorn, H. and P. Czermak, *Biotechnology of Food and Feed Additives*. 2014: Springer Berlin Heidelberg.
14. Kuenz, A., et al., *Microbial production of itaconic acid: developing a stable platform for high product concentrations.* Applied Microbiology and Biotechnology, 2012. **96**(5): p. 1209-1216.
15. Saha, B., M. Fan, and J. Wang, *Sustainable Catalytic Processes*. 2015: Elsevier Science.
16. Efe, Ç., *Recovery of Succinic Acid for Bio-based C4 Bifunctional Building Block Production*, in *Biotechnology Department*. 2011, Technische Universiteit Delft: Nederlands.
17. Agency, U.S.E.P., *Waste and Cleanup Risk Assessment Glossary.*
18. Kumar, A. and A. Awasthi, *Bioseparation Engineering*. 2009: I. K. International Publishing House.
19. Allen, S.J., G. McKay, and J.F. Porter, *Adsorption isotherm models for basic dye adsorption by peat in single and binary component systems.* Journal of Colloid and Interface Science, 2004. **280**(2): p. 322-333.
20. Limousin, G., et al., *Sorption isotherms: A review on physical bases, modeling and measurement.* Applied Geochemistry, 2007. **22**(2): p. 249-275.
21. Ghiaci, M., et al., *Equilibrium isotherm studies for the sorption of benzene, toluene, and phenol onto organo-zeolites and as-synthesized MCM-41.* Separation and Purification Technology, 2004. **40**(3): p. 217-229.
22. Ncibi, M.C., *Applicability of some statistical tools to predict optimum adsorption isotherm after linear and non-linear regression analysis.* Journal of Hazardous Materials, 2008. **153**(1–2): p. 207-212.
23. Tsai, W.-T., et al., *Adsorption characteristics of bisphenol-A in aqueous solutions onto hydrophobic zeolite.* Journal of Colloid and Interface Science, 2006. **299**(2): p. 513-519.
24. Rabinow, B.E., et al., *Biomaterials with permanent hydrophilic surfaces and low protein adsorption properties.* J Biomater Sci Polym Ed, 1994. **6**(1): p. 91-109.
25. Nam, S.W., et al., *Adsorption characteristics of selected hydrophilic and hydrophobic micropollutants in water using activated carbon.* J Hazard Mater, 2014. **270**: p. 144-52.

26.     Foo, K.Y. and B.H. Hameed, *Insights into the modeling of adsorption isotherm systems.* Chemical Engineering Journal, 2010. **156**(1): p. 2-10.

27.     Karadag, D., et al., *A comparative study of linear and non-linear regression analysis for ammonium exchange by clinoptilolite zeolite.* J Hazard Mater, 2007. **144**(1-2): p. 432-7.

28.     Han, R., et al., *Study of equilibrium, kinetic and thermodynamic parameters about methylene blue adsorption onto natural zeolite.* Chemical Engineering Journal, 2009. **145**(3): p. 496-504.

29.     Freundlich, H.M.F., *Over the Adsorption in Solution.* Journal of Physical Chemistry. **57**: p. 385-470.

30.     Adamson, A.W., *Physical chemistry of surfaces.* 1990: Wiley.

31.     Zeldowitsch, J., *Adsorption site energy distribution.* Acta Phys. Chim., 1934: p. 961–973.

32.     Haghseresht, F. and G.Q. Lu, *Adsorption Characteristics of Phenolic Compounds onto Coal-Reject-Derived Adsorbents.* Energy & Fuels, 1998. **12**(6): p. 1100-1107.

33.     Vijayaraghavan, K., et al., *Biosorption of nickel(II) ions onto Sargassum wightii: Application of two-parameter and three-parameter isotherm models.* Journal of Hazardous Materials, 2006. **133**(1–3): p. 304-308.

34.     Kundu, S. and A.K. Gupta, *Arsenic adsorption onto iron oxide-coated cement (IOCC): Regression analysis of equilibrium data with several isotherm models and their optimization.* Chemical Engineering Journal, 2006. **122**(1–2): p. 93-106.

35.     Pérez-Marín, A.B., et al., *Removal of cadmium from aqueous solutions by adsorption onto orange waste.* Journal of Hazardous Materials, 2007. **139**(1): p. 122-131.

36.     Günay, A., E. Arslankaya, and İ. Tosun, *Lead removal from aqueous solution by natural and pretreated clinoptilolite: Adsorption equilibrium and kinetics.* Journal of Hazardous Materials, 2007. **146**(1–2): p. 362-371.

37.     *R. Sips, Combined form of Langmuir and Freundlich equations, J. Chem. Phys. 16 (1948) 490–495.*

38.     Toth, J., *State equations of the solid gas interface layer.* Acta Chem. Acad. Hung. **69**: p. 311-317.

39.     M. Horsfall, A.I.S., *Equilibrium sorption study of Al3+, Co2+ andAg2+ in aqueous solutions by fluted pumpkin (Telfairia occidentalis HOOK) waste biomass.* Acta Chim, 2005: p. 174-181.

40.     Redlich, O.J.P., D.L.  J., *A useful adsorption isotherm.* Phys. Chem, 1959. **63**: p. 1024–1026.

41.     Bowen, T.C. and L.M. Vane, *Ethanol, acetic acid, and water adsorption from binary and ternary liquid mixtures on high-silica zeolites.* Langmuir, 2006. **22**(8): p. 3721-7.

42.     Nisenbaum, A., A. Apelblat, and E. Manzurola, *Volumetric properties of itaconic acid aqueous solutions.* The Journal of Chemical Thermodynamics, 2012. **47**(0): p. 42-47.

43.     Tvrdík, J., I. Křivý, and L. Mišík, *Adaptive population-based search: Application to estimation of nonlinear regression parameters.* Computational Statistics and Data Analysis, 2007. **52**(2): p. 713-724.

44.     Yaneva, Z.L., B.K. Koumanova, and N.V. Georgieva, *Linear and Nonlinear Regression Methods for Equilibrium Modelling of p-Nitrophenol Biosorption by Rhizopus oryzae: Comparison of Error Analysis Criteria.* Journal of Chemistry, 2013. **2013**: p. 10.

45.     Kumar, K.V., K. Porkodi, and F. Rocha, *Isotherms and thermodynamics by linear and non-linear regression analysis for the sorption of methylene blue onto activated carbon: Comparison of various error functions.* Journal of Hazardous Materials, 2008. **151**(2–3): p. 794-804.

46.     Kalinowski, P., *Understanding Confidence Intervals (CIs) and Effect Size Estimation.* Association for Psychological Science Observer, April 10, 2010. **23**.

47.     *Minitab 17 Statistical Software.* 2015, Minitab, Inc. p. State College.

48.     Hui, Y.H., *Handbook of Food Science, Technology, and Engineering.* 2006: Taylor & Francis.

49.     Suzuki, M., *Adsorption Engineering.* 1990. 306.

50.     Piccin, J.S., G.L. Dotto, and L.A.A. Pinto, *Adsorption isotherms and thermochemical data of FD&C Red n° 40 binding by Chitosan.* Brazilian Journal of Chemical Engineering, 2011. **28**: p. 295-304.

51.     Bulut, E., M. Özacar, and İ.A. Şengil, *Adsorption of malachite green onto bentonite: Equilibrium and kinetic studies and process design.* Microporous and Mesoporous Materials, 2008. **115**(3): p. 234-246.

52. Kaminsky, R.D. and P.A. Monson, *An analysis of the statistical model adsorption isotherm.* AIChE Journal, 1992. **38**(12): p. 1979-1989.

53. Gu, B.H., et al., *Aqueous two-phase system: An alternative process for recovery of succinic acid from fermentation broth.* Separation and Purification Technology, 2014. **138**(0): p. 47-54.

54. Belhachemi, M. and F. Addoun, *Comparative adsorption isotherms and modeling of methylene blue onto activated carbons.* Applied Water Science, 2011. **1**(3-4): p. 111-117.

55. Agency, U.S.E.P., *Definition of Adsorption*, W.a.C.R. Assessment, Editor. 2015.

56. Yan, F., et al., *Determination of Adsorption Isotherm Parameters with Correlated Errors by Measurement Error Models.* Chemical Engineering Journal.

57. Cheng, K.-K., et al., *Downstream processing of biotechnological produced succinic acid.* Applied Microbiology and Biotechnology, 2012. **95**(4): p. 841-850.

58. Gök, A., et al., *Equilibrium, kinetics and thermodynamic studies for separation of malic acid on layered double hydroxide (LDH).* Fluid Phase Equilibria, 2014. **372**: p. 15-20.

59. Yan, Q., et al., *Fermentation process for continuous production of succinic acid in a fibrous bed bioreactor.* Biochemical Engineering Journal, 2014. **91**(0): p. 92-98.

60. contributors, W., *Gauss–Newton algorithm*, in *Wikipedia, The Free Encyclopedia*. 2015.

61. *GraphPad Curve Fitting Guide*. 2015.

62. Sheskin, D., *Handbook of Parametric and Nonparametric Statistical Procedures*. 2000. 1016.

63. Klement, T. and J. Büchs, *Itaconic acid – A biotechnological process in change.* Bioresource Technology, 2013. **135**: p. 422-431.

64. chemistry, C.S.a.s., *Itaconic acid data*.

65. Kuhn, R.C., M.A. Mazutti, and F.M. Filho, *Kinetic and mass transfer effects for adsorption of glucose, fructose, sucrose and fructooligosaccharides into X zeolite.* LWT - Food Science and Technology, 2012. **48**(1): p. 127-133.

66. Ruthven, D.M., *Principles of Adsorption and Adsorption Processes*. 1984. 464.

67. Song, H. and S.Y. Lee, *Production of succinic acid by bacterial fermentation.* Enzyme and Microbial Technology, 2006. **39**(3): p. 352-361.

68. Yeh, Y.-L., *Real-time measurement of glucose concentration and average refractive index using a laser interferometer.* Optics and Lasers in Engineering, 2008. **46**(9): p. 666-670.

69. López-Garzón, C.S. and A.J.J. Straathof, *Recovery of carboxylic acids produced by fermentation.* Biotechnology Advances, 2014. **32**(5): p. 873-904.

70. Francisco, M., et al., *Recovery of glucose from an aqueous ionic liquid by adsorption onto a zeolite-based solid.* Chemical Engineering Journal, 2011. **172**(1): p. 184-190.

71. Grieco, S.A. and B.V. Ramarao, *Removal of TCEP from aqueous solutions by adsorption with zeolites.* Colloids and Surfaces A: Physicochemical and Engineering Aspects, 2013. **434**(0): p. 329-338.

72. Boulinguiez, B., P. Le Cloirec, and D. Wolbert, *Revisiting the Determination of Langmuir Parameters—Application to Tetrahydrothiophene Adsorption onto Activated Carbon.* Langmuir, 2008. **24**(13): p. 6420-6424.

73. Ho, Y.-S., *Selection of optimum sorption isotherm.* **42**: p. 2113-2130.

74. Efe, Ç., et al., *Separation of succinic acid from its salts on a high-silica zeolite bed.* Chemical Engineering and Processing: Process Intensification, 2011. **50**(11–12): p. 1143-1151.

75. Efe, Ç., L.A.M. van der Wielen, and A.J.J. Straathof, *Techno-economic analysis of succinic acid production using adsorption from fermentation medium.* Biomass and Bioenergy, 2013. **56**(0): p. 479-492.

76. Atav, R., *Thermodynamics - Fundamentals and Its Application in Science*, in *Thermodynamics of Wool Dyeing*, R. Morales-Rodriguez, Editor. 2012, InTech. p. 554.

77. Medicine, U.S.N.L.o., *TOXNET Toxicology Data Network, Fumaric Acid*.